

**SPECTROSCOPIC
AND
STRUCTURAL PROPERTIES
OF
TTBC J-AGGREGATES**

**A THESIS
SUBMITTED TO THE DEPARTMENT OF
CHEMISTRY
AND THE INSTITUTE OF ENGINEERING AND
SCIENCE OF BILKENT UNIVERSITY
IN PARTIAL FULFILLMENT OF THE
REQUIREMENTS FOR THE DEGREE OF
MASTER OF SCIENCE**

**BY
BURAK BIRKAN
JUNE, 2002**

I certify that I have read this thesis and that in my opinion it is fully adequate, in scope and in quality, as a thesis for the degree of Master of Science.

Asst. Prof. Dr. Serdar Özçelik (Supervisor)

I certify that I have read this thesis and that in my opinion it is fully adequate, in scope and in quality, as a thesis for the degree of Master of Science.

Prof. Dr. Şefik Süzer

I certify that I have read this thesis and that in my opinion it is fully adequate, in scope and in quality, as a thesis for the degree of Master of Science.

Assoc. Prof. Dr. Ulrike Salzner

I certify that I have read this thesis and that in my opinion it is fully adequate, in scope and in quality, as a thesis for the degree of Master of Science.

Asst. Prof. Dr. Ahmet Oral

I certify that I have read this thesis and that in my opinion it is fully adequate, in scope and in quality, as a thesis for the degree of Master of Science.

Prof. Dr. Demet Gülen

Approved for the Institute of Engineering and Science:

Prof. Dr. Mehmet B. Baray

Director of the Institute of Engineering and Science

ABSTRACT

SPECTROSCOPIC AND STRUCTURAL PROPERTIES OF TTBC J-AGGREGATES

Burak Birkan

M.S. in Chemistry

Supervisor: Asst. Prof. Dr. Serdar Özcelik

June, 2002

The aim of this thesis is to investigate the spectroscopic and structural properties of the TTBC J-aggregates. Absorption, emission and excitation spectroscopy techniques are used to study the properties of the J-aggregates of 1,1',3,3'-tetrachlorobenzimidazolocarboyanine (TTBC). The dependence of absorption spectra on dye and ion concentration was investigated. A model is presented to explain the asymmetrical splitting. The interaction between molecules was found to be affected by the intermolecular distance, the orientation of the molecules and the size of the aggregate chain.

Keywords: TTBC, J-aggregate, Molecular Exciton Theory, Absorption Spectrum Simulation, Asymmetrical Davydov Splitting

ÖZET

TTBC J-KÜMELERİN SPEKTROSKOPİK VE YAPISAL ÖZELLİKLERİ

Burak Birkan

Kimya, Yüksek Lisans

Tez Yöneticisi: Asst. Prof. Dr. Serdar Özcelik

Haziran, 2002

Bu tezin amacı, TTBC J-kümelerin yapısal ve spektroskopik özelliklerini incelemektir. Soğurma, Floresans Uyarma ve Işıma Spektroskopisi teknikleri kullanılarak 1,1',3,3'-tetrachlorobenzimidazolocarbocyanine (TTBC) adlı sayanın boyasının oluşturduğu J-kümelerin özellikleri incelenmiştir. Soğurma spektrumunun boya ve iyon konsantrasyonuna bağlı olarak değiştiği gözlenmiştir. Soğurma spektrumu asimetrik eksiton band yarılması göstermektedir. Simetrik olmayan eksiton band yarılması önerilen bir model yardımı ile incelenerek; spektroskopik özelliklerin yapısal parametrelerle nasıl değiştiği belirlenmiştir. Moleküller arası etkileşimin uzaklığa, moleküllerin yönelimlerine ve kümelenmenin boyuna bağlı olduğu ortaya konmuştur.

Anahtar Kelimeler: TTBC, J-kümeler, Moleküler Eksiton Teorisi, Soğurma Spektrumu Similasyonu, Asimetrik Davydov Yarılması

ACKNOWLEDGMENT

This thesis owes its existence to the help, support, and inspiration of many people. First of all I am very thankful to my advisor Asst. Prof. Dr. Serdar Özçelik without whose support this thesis would not have been possible. He carefully guided me throughout the pursuit of my Master's degree at Bilkent University. Her ideas and suggestions have been invaluable to this thesis.

I would like to thank Prof. Dr Demet Gülen for helping me throughout the theoretical part of this thesis and for many hours of mind-opening discussions.

I would like to thank Prof. Dr. Şefik Süzer, Assoc. Prof. Dr. Ulrike Salzner and Asst. Prof. Dr. Ahmet Oral for their readiness to read this text and evaluate my work.

Many thanks to my colleague Onur Atasoylu and all other friends at Bilkent for their insightful suggestions and assistance at every stage of my work.

I owe special gratitude to my family for continuous and unconditional support of all my undertakings, scholastic and otherwise.

Finally, I would like to thank my fiancée Tuğba for endless love and support.

TABLE OF CONTENTS

Abstract	iv
Özet	v
Acknowledgement	vi
Table of Contents	vii
List of Figures	ix
Chapter 1 Introduction	1
1.1 Introduction	1
1.2 Molecular Aggregates	4
Chapter 2 The Molecular Extinction Model	
2.1 Introduction	8
2.1.1 Molecular Dimers	10
2.1.2 Infinite Linear Polymer	11
2.2 The Intermolecular Interaction Potential	12
2.3 Spectral and Structural Properties of Cofacial Parallel Dimers	13
2.3.1 The Extinction Band Width	14
2.3.2 Spectral properties of Dimers	16

2.4 Spectral and Structural Properties of Linear Chain Aggregates	17
Chapter 3 Spectroscopic and Structural Properties of a Benzimidazolocarboyanine Dye In Aqueous Solutions	
3.1 Introduction	21
3.2 Experimental	22
3.2.1 Effect of NaOH Concentration on Aggregation	25
3.2.2 Effect of TTBC Concentration on Aggregation	27
3.2.3 Fluorescence Emission and Excitation Spectroscopy	31
Chapter 4 Computational and Theoretical Work	
4.1 Introduction	33
4.2.1 Interaction Energy and Size Dependency of Absorption Spectrum for J-band and H-band for Single Chain	35
4.2.2 Molecular Orientation and Intermolecular Distance Dependency of Absorption Spectrum for J-band and H-band for Single Chain	37
4.3 Single Chain Dependency on Molecular Structure	38
Chapter 5 Conclusion	47
References	49

LIST OF FIGURES

1.1	Molecular representations of TTBC and PIC	3
1.2	The energy level diagram for a monomer and dimers shows that the allowedness for dimer transitions from the ground state (G) to the split excited states (E)	6
2.1	Structure and coordinates of parallel or card pack dimer	10
2.2	Schematic energy level diagram showing exciton splitting in molecular dimers	15
2.3	Schematic diagram showing selection rules and luminescence properties of a parallel (card-pack) dimer compared to monomer	16
2.4	Structure (A), and energy levels (B) of long chain aggregates in which the molecular components are translatory equivalent	18
2.5	Structure (A), and energy levels (B) of alternate transitional aggregate in which every other molecular component is translatory equivalent	19
3.1	Chemical structure of TTBC	21
3.2	Absorption Spectrum of TTBC in methanol	24
3.3	Absorption Spectrum of TTBC in aqueous solution. M-band belongs to monomer and J-band arises from J-aggregate	24
3.4	Absorption Spectrum of TTBC in aqueous solution. H-band and J-band	25
3.5	Absorption spectra of TTBC/NaOH aqueous solutions for different NaOH concentrations. [TTBC] = 1×10^{-4} M in methanol.	26

3.6	The change of the absorption spectrum of TTBC/NaOH aqueous solutions for different TTBC concentrations. [NaOH]=0.01M	27
3.7	Normalized absorption spectra of TTBC in aqueous solution, [NaOH] =0.01 M-1	28
3.8	Normalized absorption spectra of TTBC in aqueous solution, [NaOH] =0.01 M-2	29
3.9	The change of the absorption spectrum of TTBC/NaOH aqueous solutions for different TTBC concentrations. [NaOH] = 0.01M	30
3.10	Absorption and fluorescence spectra of TTBC in methanol at room temperature. [TTBC = 1×10^{-5} M]..	31
3.11	Fluorescence spectrum of TTBC/NaOH aqueous solution ..	32
4.1	The J-band absorption maximum as a function of interaction energy (ϵ), and number of molecules forming the aggregate (N)	35
4.2	The H-band absorption maximum as a function of interaction energy (ϵ), and number of molecules forming the aggregate (N)	36
4.3	Molecular orientation and intermolecular distance dependency of absorption spectrum for J-band	37
4.4	Molecular orientation and intermolecular distance dependency of absorption spectrum for H-band	38
4.5	Representative scheme for an aggregate chain	38
4.6	Change of orientation of H-band with respect to J-band ...	39
4.7	Change of intermolecular distance with respect to molecular orientation as a function of interaction energy for J-band	40
4.8	Change of intermolecular distance with respect to molecular orientation as a function of interaction energy for H-band	40
4.9	Coupling of two different chains	41
4.10	The interaction geometry for the chains.	41

4.11	The change of the absorption spectrum of TTBC/NaOH aqueous solutions for different TTBC concentrations. [NaOH] = 0.01M.	43
4.12	The change of the absorption spectra with respect to the mutual orientation of the molecules forming J- and H-aggregate. .	44
4.13	The change of the absorption spectra with respect to the distance between the molecules	45

CHAPTER 1

INTRODUCTION

1.1. INTRODUCTION

Presently, there is considerable interest in the optical properties of the nanostructured materials such as quantum-wells and -dots ^[1], Langmuir Blodgett films ^[2, 3], polymers and molecular aggregates ^[2-6]. As intermediates between single molecules and bulk phases, these systems are ideal to investigate the changes of photophysical properties between these two extremes due to their low dimensionality and discreteness induced by the confinement.

Among these materials, there is a group known as molecular aggregates. Molecular aggregates were discovered by Gunter Scheibe and Edwin E. Jelley in the late 1930s ^[4, 5]. Scheibe attributed the peculiar spectroscopic behavior to reversible polymerization of the chromophores due to intermolecular interactions.

The optical properties of molecular aggregates differ strongly from single molecules and from crystalline systems. Electrostatic intermolecular

interactions in the aggregate couple optical transition on different molecules. In general, the strength of this coupling depends on the size of the transition dipole moment, intermolecular distance, mutual intermolecular orientation and geometry ^[6, 7], and intensity (oscillator strength) of light absorption by the component molecule. Through this coupling an optical excitation on a particular molecule can be transferred to other molecules in the aggregate, i.e., the excitation becomes delocalized. The rate of this transfer is related to the coupling strength ^[8]. If the excitation transfer occurs on a much faster timescale than other dynamical processes, it will occur coherently and the eigenstates are best described as collective states – excitons - of the aggregate.

The explanation for the observed absorption spectrum came from the molecular exciton theory, which was first formulated by Frenkel ^[9]. Lately, the exciton model, which explains the spectral properties of inorganic semiconductors and ionic crystals, was developed by Wannier^[10], and Mott ^[11]; then Knox ^[12] showed that both models are limiting cases of a general description of excitations in a crystal.

The molecular dye aggregates play an important role in many technological applications such as spectral sensitizers in photography^[13]. These systems are also found in biological systems where most photobiological processes, including photosynthesis, rely on aggregates for energy or charge transfer processes. Dye aggregates adsorbed onto silver halide semiconductor substrates have found extensive use as spectral sensitizers to inject electrons into semiconductors, the resultant mobile electrons can lead to important processes and reactions in solar cells and photographic systems. Recently, molecular aggregates- particularly J-aggregates- have drawn attention due to their nonlinear optical properties and superradiant behavior ^[14-21].

The aim of the scientists now is to characterize and understand the optical and physical properties of J-aggregates in order to optimize their use for the future technical and scientific applications.

The subject of this dissertation is to investigate the spectroscopic and structural properties of J-aggregates in various environments. In this study a cyanine dye (Figure 1), 1,1',3,3'-tetraethyl-5,5',6,6'-tetra-chloro benzimidazolocarbo-cyanine (TTBC) was used. Absorption, excitation and emission spectroscopy techniques were applied. A computational work was also carried out to enhance our understanding on structural effects on optical properties.

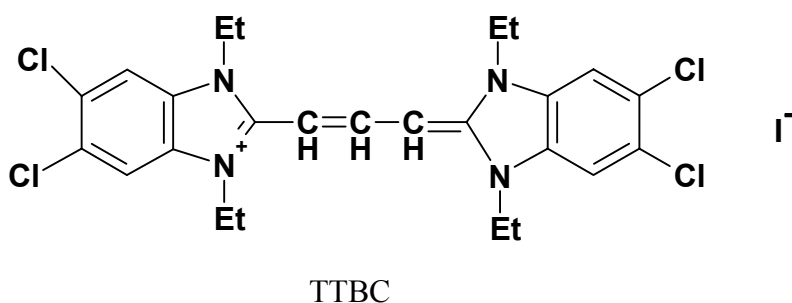


Figure 1.1. Molecular representation of TTBC.

This thesis is organized as follows:

A synopsis on molecular aggregates is provided in the introduction chapter.

Chapter 2 is a review of the molecular exciton theory for molecular aggregates, which summarizes –in general- structural and spectral properties of aggregates

Spectroscopic and structural properties of 1,1',3,3'-tetraethyl-5,5',6,6'-tetrachloro benzimidazolocarboyanine (TTBC) aggregates are presented in Chapter 3 .

1.2. MOLECULAR AGGREGATES (A brief introduction)

Numerous investigations of organic dyes showed that in aqueous solution they can appear in a variety of different aggregation and fluorescence spectra. In general three types of aggregation states can be distinguished. Besides the monomer band, characterized by the so-called M-band, dimers (D-band) and higher aggregated species like H- or J-aggregates can be formed. Contrary to H-aggregates, which have an absorption peak blue shifted compared to the M-band, J-aggregates, which were invented by Scheibe and Jelley in the late 1930 s ^[4,5], have an intense, narrow and red-shifted absorption band.

Upon aggregation, the major spectral changes that have been observed experimentally are (a) a displacement of emission and absorption bands relative to the monomer bands, (b) a splitting of spectral lines with a corresponding change in the polarization properties, (c) a variation of selection rules, (d) changes in molecular vibrational frequencies and the introduction of intermolecular lattice modes ^[21].

Deviations from Beer's law with the appearance of H- or J -bands have been rationalized in terms of dye aggregation, i.e., Forster first interpreted the formation of dimers, trimers, and n-mers, and the accompanying spectral changes with a classical oscillator model. Subsequent treatments explained these spectral manifestations of dye/dye interactions with the theory of energetically delocalized states, i.e., excitons, which had been applied by Davydov to spectra of molecular crystals ^[22] According to this treatment, the excitation achieved in a single

molecule of a periodic molecular assembly is transferred by coupled oscillation from a molecule to another in a period, which is shorter than the vibration time of the component molecules in the assembly.

It is instructive to consider the McRae-Kasha exciton model for the case of dimeric molecules ^[23]. As shown schematically in Figure 1.2, it is assumed that molecular axis, parallels its transition polarization axis, i.e., the transition dipole is placed along the long axis of the molecule. Upon excitation of the dimer from its ground state (G), the model provides a splitting of the excited state (E) because of electronic degeneracy. Whether a transition is allowed to the lower or the higher excited state depends on the angle (α) between the transition dipoles and the aggregate axis. The ground states of the monomeric and dimeric molecules are shown in Figure 1.2 are fixed at the same relative position, although the point-multipole expansion employed by Kasha provides for a displacement of the dimer ground state because of van der Waals interaction. Judging from the effect of dye aggregation on ground state properties such as infrared transitions, redox potential and basicity -the latter is particularly strongly depressed by J-aggregation -a common ground state is an oversimplification ^[24-26].

However, excitonic interactions can be conveniently discussed in terms of energies normalized to a common ground state. Thus, Figure 1.2 shows that when the transition dipoles are in line with the molecular axis of the dimer, i.e., when $\alpha = 0$, then the transition to the lower excited level will be allowed and consequently the maximum absorption of the dimer will be red-shifted relative to the absorption of the monomer.

In fact, according to the Kasha's approximation ^[23] a red shift, as observed in J-band formation, will occur as long as the angle α is less than about 54.7° , which was called as magic angle. If α is greater than that

value, the transition to the higher excited level will be allowed so that the spectral band will be blue-shifted relative to the monomeric dye.

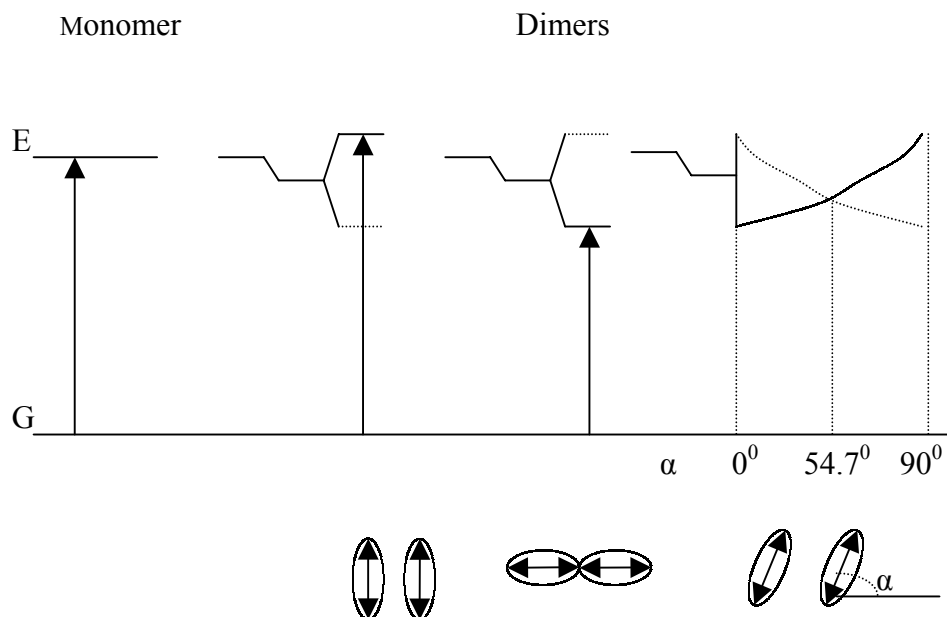


Figure 1.2. The energy level diagram for a monomer and dimers shows that the allowedness for dimer transitions from the ground state (G) to the split excited states (E).

In J-aggregates, transition only to the low energy states of the exciton band is allowed and, as a consequence, J-aggregates are characterized by a high fluorescence quantum yield. In contrast, after exciting the upper exciton band, a rapid downward energy relaxation to the lower exciton states occurs that exhibits vanishingly small transition dipole moments. Therefore, their fluorescence is suppressed and a low fluorescence yield characterizes blue-shifted spectra arising from H-aggregates.

Intermolecular interactions in J-aggregates couple optical transitions of different molecules, which depends on the size of the

transition dipole moment, the intermolecular distances and the orientation of the molecules ^[27-30]. An optical excitation can be transferred to other molecule of the aggregate due to coupling. Strong coupling between the molecules leads to delocalization of the excitation, whereas disorder in the couplings between the molecules and/or in the single molecule energies counteracts the exciton delocalization. The degree of delocalization is determined by the relative magnitude of the intermolecular coupling, compared to the energetic disorder ^[16, 31]. The dynamics of the system may be a combination of the limiting cases: the excitation can be delocalized over a small part of the system which behaves as an exciton, while, on a larger scale the excitation is transferred along the aggregate as the incoherent case. In the coherent case, the excitation is transferred along the aggregate is faster time than other dynamic processes (such as dephasing and spontaneous emission) in the system. The molecular aggregate behaves as a giant molecule, exhibiting superradiant emission and giant optical nonlinearities^[16].

CHAPTER 2

THE MOLECULAR EXCITON MODEL

2.1. INTRODUCTION

Excited electronic states of molecular aggregates can be described using the molecular exciton model. This chapter reviews the theory of molecular excitons.

The energy of interaction between molecules, weak as it may be, imposes a communal response upon the molecular behavior in the aggregate; the collective response is embodied in an entity called an exciton. This quasi-particle was initially introduced by Frenkel^[9, 32] and was generalized by Wannier^[10] and Peierls.

The first experimental investigations of excitons in molecular crystals were carried out around 1930. Davydov was the first who developed the molecular exciton theory for molecular crystals^[22]. At the same time excitonic features were discovered in the absorption spectra of highly concentrated solutions of pseudoisocyanine dye molecules^[4, 30].

The molecular exciton model, which is applicable to van der Waals crystals (e.g., polyenes and rare-gas solids) and accounts reasonably well for the spectral similarities and differences observed between individual molecules and their aggregate form. The molecular exciton model offers a theoretical method for treating the resonance interaction of excited states of weakly coupled composite systems.

The molecular exciton model provides a satisfactory approximation for the treatment of excited states. Intermolecular (or interchromophore) electron overlap and electron exchange are negligible. In such systems the optical electrons associated with individual component molecules (or chromophoric units) are considered localized, and the molecular units (or chromophoric units) preserve their individual characteristics in the aggregate system, with relatively slight perturbation. The mathematical formalism then takes the form of a state interaction theory, with the exclusion of details of atomic orbital composition usual in molecular electronic theories. The electronic states of the aggregate are then expressed in terms of the electronic states of the component light absorbing units.

The starting point in the molecular exciton model treatment will be the singlet electronic energy states and their corresponding electronic state wave functions for a component molecule of the molecular aggregate. It is assumed that the electronic singlet state energies $E_0, E_1, E_2, E_3, \dots$ and the corresponding wave functions $\psi_0, \psi_1, \psi_2, \psi_3, \dots$ are known, satisfying the individual molecule's Schrödinger equation

$$H_n\psi_n = E_n\psi_n \quad (2.1)$$

In general, each problem will involve only a pair of states and wave functions, so these may be designated G and E for ground and excited singlet state energy, and ψ_u , and ψ_u^\dagger for the corresponding state

wave functions for molecule u . All molecules of an aggregate will be considered to be identical. Many specific cases will be discussed as an individual base. The purpose of this section is to provide a background for the reader.

2.1.1. Molecular Dimers

The ground state wave function for a molecular dimer consisting of two identical molecules will be (Figure 2.1)

$$\Psi_G = \psi_u \psi_v \quad (2.2)$$

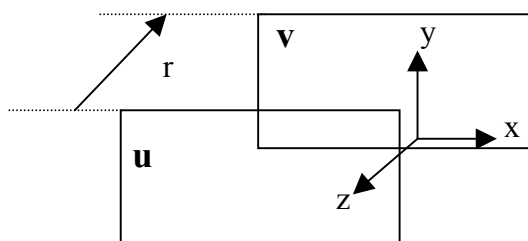


Figure 2.1. Structure and coordinates of parallel or card pack dimer.

This is the unique ground state wave function of the dimer. It is totally symmetric with respect to all symmetry operations of the dimer. The first excited state of the dimer can be described equally well by two possible wave functions

$$\Phi_1 = \psi_u \psi_v^\dagger \text{ and } \Phi_2 = \psi_u^\dagger \psi_v. \quad (2.3)$$

These are degenerate and do not describe stationary states of the system. The correct zero order wave functions are

$$\Psi_I = \frac{1}{\sqrt{2}} (\Phi_1 + \Phi_2) = \frac{1}{\sqrt{2}} (\psi_u \psi_v^\dagger + \psi_u^\dagger \psi_v) \quad (2.4)$$

$$\Psi_{II} = \frac{1}{\sqrt{2}} (\Phi_1 - \Phi_2) = \frac{1}{\sqrt{2}} (\psi_u \psi_v^\dagger - \psi_u^\dagger \psi_v)$$

Interchange of molecular labels u , v indicates that the first function is totally symmetric and the second is antisymmetric. In both of the

stationary state exciton states Ψ_I and Ψ_{II} , the excitation is on both molecules, u and v , i.e., the excitation is collective or delocalized.

2.1.2. Infinite Linear Polymer

It is instructive to consider a simple linear chain or array of molecules forming a thread-like polymer as a model for development of the exciton treatment for multimolecular aggregates.

Assuming N identical molecules (where N is very large or nearly infinite) in a linear array, the ground state wave function will be unique, totally symmetric wave function

$$\Psi_G = \psi_1 \psi_2 \psi_3 \dots \psi_a^\dagger \dots \psi_N = \prod_{n=1}^N \psi_n \quad (2.5)$$

The lowest-energy singlet excited state of the aggregate can be represented by the wave function

$$\Phi_a = \psi_a^\dagger \prod_{n=1}^N \psi_n = \psi_1 \psi_2 \psi_3 \dots \psi_a^\dagger \dots \psi_N \quad (a = 1, 2, 3 \dots N) \quad (2.6)$$

where ψ_a^\dagger indicates that the molecule a is in its lower singlet excited state, and the remaining molecules are in their ground states. There are N such product functions Φ_a , i.e., these functions are N -fold degenerate, and they correspond to nonstationary states of the excited aggregate.

Symmetry adapted linear wave functions of the N wave functions Φ_i can be taken in order to get stationary exciton states of the aggregate. In general, the k^{th} exciton stationary state wave function can be described by

$$\Psi_k = \frac{1}{\sqrt{N}} \sum_{a=1}^N C_{ak} \Phi_a \quad (2.7)$$

where $|C_{ak}|^2$ determines the probability that the a^{th} molecule is excited.

Assuming ideal periodic distribution of molecules with one molecule per unit cell, N being very large so that each molecule will have

modulus unity for excitation, the various coefficients C_{ak} will differ only in their phase factors, and the wave function may be written

$$\Psi_k = \frac{1}{\sqrt{N}} \sum_{a=1}^N e^{2\pi i k a / N} \Phi_a \quad (k = 0, +1, -1, +2, N/2) \quad (2.8)$$

As in the dimer case, the N exciton stationary state wave functions show (a) collective excitation of molecular units of the aggregate, and (b) orthogonality of the stationary states.

2.2. THE INTERMOLECULAR INTERACTION POTENTIAL

The energy states and wave functions for a molecular aggregate are determined by adding to the total Hamiltonian for the collection of unperturbed molecules a term $\sum_{l,k < l} V_{kl}$ where V_{kl} is the intermolecular interaction operator acting between molecules k and l , and the summation is carried over all pairs of molecules. This is essentially an intermolecular coulombic potential term, representing the interactions between charged particles (electronic and nuclei) on the two molecules [33]. However, the use of an exact coulombic potential, V_{coul} , would involve $1/r_{kl}$ as an operator (r_{kl} is the kl intermolecular distance), which would make simplification of the interaction integrals impossible. Accordingly, a point-multipole expansion is used:

$$V_{coul} = V_{mono-mono} + V_{mono-di} + V_{di-di} + V_{quad-quad} + V_{di-quad} + V_{octu-octu} \quad (2.9)$$

For neutral total charge distribution the monopole interactions are zero. For allowed electric-dipole transitions, the dipole-dipole potential term becomes the leading one and higher multipoles are neglected.

Thus, for strong absorption bands, corresponding to allowed electric dipole transitions

$$V_{coul} \cong V_{dipole-dipole} = -\frac{e^2}{r_{kl}^3} \sum_{i,j} (2z_k^i z_l^j - x_k^i x_l^j - y_k^i y_l^j) \quad (2.10)$$

where r_{kl} is the distance between the point dipoles in the molecules k and l , and x_k^i is the x coordinate of the i^{th} electron on molecule k , x_l^j is the x coordinate of the j^{th} electron on molecule l , and so forth. The coordinate system is chosen with the z -axis parallel to the line of molecular centers. The summation is over all electrons in each molecule.

Thus, an approximation has been introduced which allows the physical interpretation that the excited state resonance splitting arises from the electrostatic interaction of transition electric dipoles on neighboring molecules. In most cases, electron displacement along one coordinate is effected by the light wave causing the excitation at particular frequency, so that, in general, only one term in the dipole-dipole interaction may remain.

For the lowest state of an x-polarized transition in a dimer consisting of two molecules u and v , whose transition moments are both parallel to the x -axis, the perturbation potential reduces to

$$V_{uv} = -\frac{e^2}{r_{kl}^3} \sum_{i,j} (x_k^i x_l^j) \quad (2.11)$$

2.3. SPECTRAL AND STRUCTURAL PROPERTIES OF COFACIAL PARALLEL DIMERS

The application of exciton formalism to the problem of molecular aggregates was made by El-Bayomi *et al* ^[34].

2.3.1. The Exciton Band Width

Spectral and structural properties of dimers can be evaluated using the Hamiltonians and wave functions discussed above for certain structural models. The energy of interaction will be given by the expectation value of the interaction potential with respect to the degenerate excited states of the dimer:

$$\varepsilon = \iint \psi_u \psi_v^\dagger V_{uv} \psi_u^\dagger \psi_v d\tau_u d\tau_v. \quad (2.12)$$

Inserting the form of the V_{uv} appropriate to an x-polarized electric-dipole transition in molecules u and v

$$\varepsilon = \frac{e^2}{r_{uv}^3} \iint \psi_u \psi_v^\dagger \left(\sum_{i,j} x_u^i x_v^j \right) \psi_u^\dagger \psi_v d\tau_u d\tau_v. \quad (2.13)$$

$$\varepsilon = \frac{1}{r_{uv}^3} \left[\int \psi_u \left(\sum_i x_u^i \right) \psi_u^\dagger d\tau_u \right] * \left[\psi_v^\dagger \sum_j x_v^j \psi_v \right] \quad (2.14)$$

Each of the integral corresponds to the transition moment integral for the excitation of the individual (monomer) molecules u and v ,

$$M_u = \int \psi_u \left(\sum_i e x_u^i \right) \psi_u^\dagger d\tau_u. \quad (2.15)$$

The phase factor of the transition moment should be considered at this point. Thus, in order to make the exciton wave stationary wavefunction, Ψ_b , corresponding to an energy, which is lower than the monomer energy by a factor of ε , the phase factor should be chosen

$$M_u = -M_v. \quad (2.16)$$

The expression for the interaction energy for the parallel dimer becomes

$$\varepsilon = -\frac{M_u^2}{r_{uv}^3} \quad (2.17)$$

By this expression, the exciton band width will be equal to twice this value or 2ε .

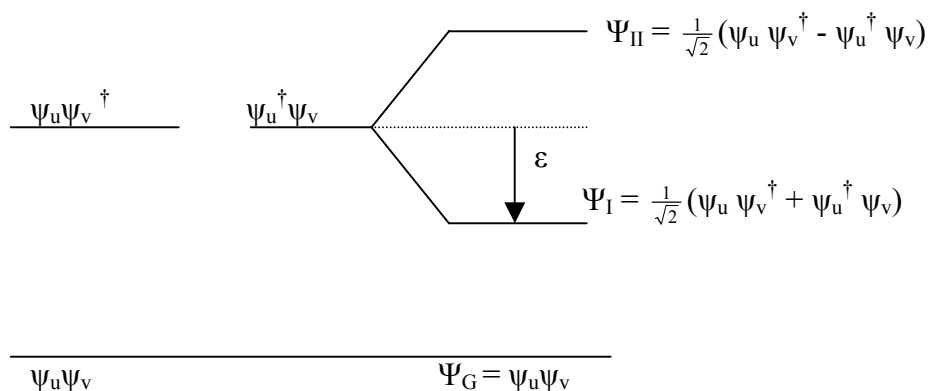


Figure 2.2. Schematic energy level diagram showing exciton splitting in molecular dimers.

For a dimer with arbitrary mutual orientations of molecular axes with respect to an x, y, z coordinate frame, the energy of interaction is given by

$$\varepsilon = -\frac{M_u^2}{r_{uv}^3} (2 \cos \theta_u^z \cos \theta_v^z - \cos \theta_u^x \cos \theta_v^x - \cos \theta_u^y \cos \theta_v^y) \quad (2.18)$$

where again M_u represents the transition moment in a free molecule, and $\cos \theta_u^x, \cos \theta_u^y, \cos \theta_u^z$ represents the cosines of the angles which the transition moment M_u for molecule u makes with the $x, y,$ and z axes.

A sample calculation of exciton splitting may be shown by using the definition of oscillator strength^[35]

$$f = 4.704 \times 10^{29} \bar{\nu} M^2 \quad (2.19)$$

where $\bar{\nu}$ is the frequency in cm^{-1} and M is the transition moment in e.s.u., the expression for ε becomes

$$\varepsilon = -\frac{f}{4.704 \times 10^{29} \bar{\nu} r^3} \quad (2.20)$$

where r may be taken as the distance between centers of the two molecules. Using $f = 1$ for a strongly allowed band at $\bar{\nu} = 20,000 \text{ cm}^{-1}$ (500 nm), the transition moment is calculated as $M \cong 10^{-17} \text{ esu.}$ or 10 Debye. Using some values of r_{uv} , the corresponding values of ε may be estimated: -870 cm^{-1} for 1 nm and -6960 for 0.5 nm.

2.3.2. Spectral Properties of Dimers

Some characteristics of the parallel dimers have been recognized in the literature. These are (a) the absorption characteristically blue-shifts by 2000-4000 cm^{-1} , (b) the fluorescence of the monomer is quenched, and (c) the relatively inefficient phosphorescence of the monomer becomes predominant.

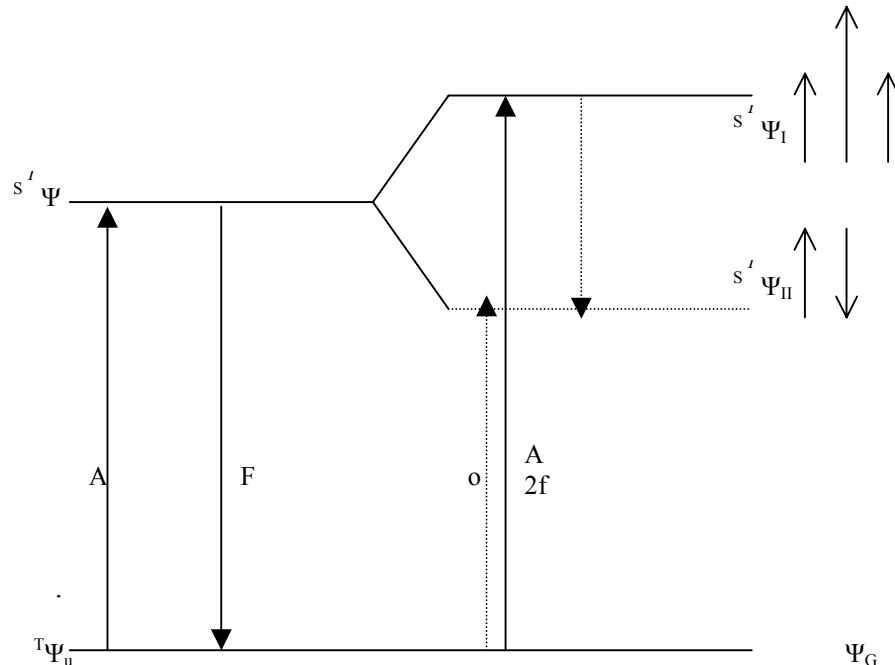


Figure 2.3. Schematic diagram showing selection rules and luminescence properties of a parallel (card-pack) dimer compared to monomer.

Figure 2.3 serves to illustrate this interpretation. In the monomer, the absorption to the lowest singlet excited state is strongly allowed, and very rapid fluorescence emission occurs with a competition of a transition to a triplet state. In the dimer, the allowed excitation state is higher in energy than the singlet excited state of the monomer: a blue shift is thus accounted for in the case of the parallel, dimer.

2.4. SPECTRAL AND STRUCTURAL PROPERTIES OF LINEAR CHAIN AGGREGATES

The exciton model will be applied to long chain linear aggregates. The exciton band width and spectral properties will be discussed. Two simple cases, that offer the best illustrations of the nature of the exciton bands in large molecular aggregates are:

Case A: A long chain aggregates in which the molecular components are translationally equivalent (Figure 2.4.A), i.e., one molecule per unit. By variation of the angle α between the molecular axis and the aggregate axis, one can go from a parallel chain aggregate to a head-to-tail chain aggregate, as α goes from $\pi/2$ to 0. In these aggregates the molecular subunits are assumed to have their optical electrons localized on each component molecule.

Case B: The alternate translational aggregate in which every other molecular component is translationally equivalent (Fig. 2.4.B), i.e., two molecules per unit.

In this model, the surroundings of neighboring molecules are equivalent, because the excited states of the aggregate are described by wavefunctions of the form of *Equation 2.8*.

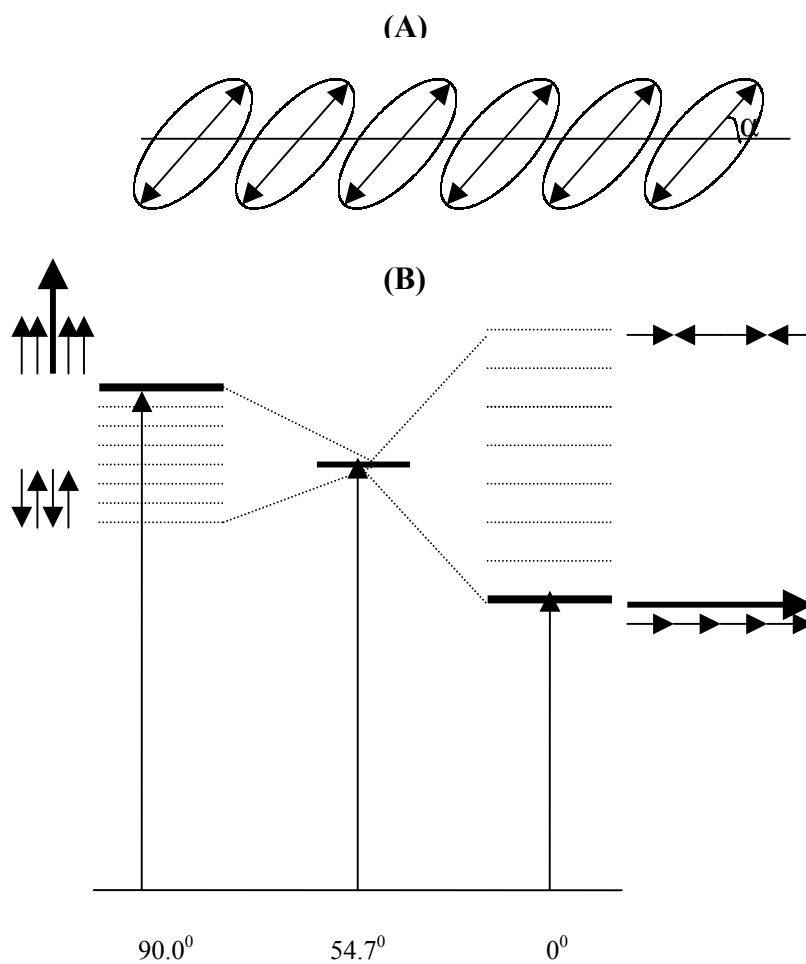


Figure 2.4. Structure (A), and energy levels (B) of long chain aggregates in which the molecular components are translatory equivalent.

The first order exciton state energies for linear chain polymer are given by ^[36, 37]

$$E_k = E_a^o + 2 \left(\frac{N-1}{N} \right) \cos \left(\frac{2\pi k}{N} \right) \varepsilon_{a,a+1} \quad (k = 0, +1, -1, +2, \dots, N/2) \quad (2.21)$$

where E_a^o denotes the energy of the first excited singlet state of a monomer of the aggregate; $\varepsilon_{a,a+1}$ represents the matrix element for the interaction between two adjacent molecules. As an approximation, only nearest neighbor interactions are considered. Thus,

$$\varepsilon_{a,a+1} = \int \Phi_a H' \Phi_{a+1} d\tau. \quad (2.22)$$

As in the case of the dimer, the phase factors for excitation are specified to make $\varepsilon_{a,a+1}$ negative for the card-pack structure. The perturbation operator H' may be taken as the appropriate form of the dipole-dipole operator.

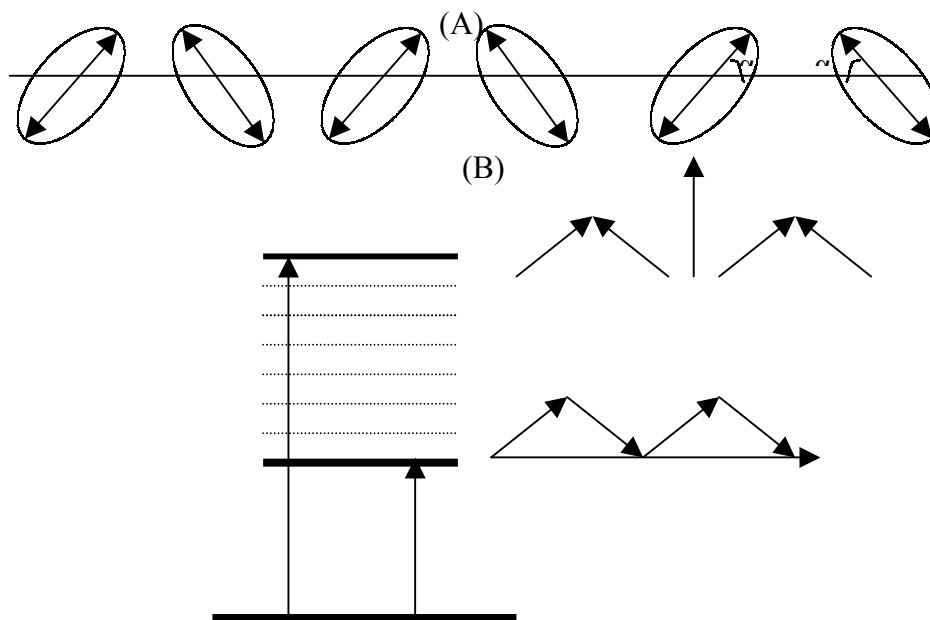


Figure 2.5. Structure (A), and energy levels (B) of alternate translational aggregate in which every other molecular component is translatory equivalent.

Two cases will be considered here for illustration purposes: (a) translational chain aggregate shown in Figure 2.4.B, and (b) alternate translational chain aggregate shown in Figure 2.5.B.

The interaction matrix element is expressed as follows:

$$\varepsilon_A = \frac{|M|^2}{r_{uv}^3} (1 - 3 \cos^2 \alpha) \text{ for case A} \quad (2.23)$$

and

$$\varepsilon_B = \frac{|M|^2}{r_{uv}^3} (1 + \cos^2 \alpha) \text{ for case B} \quad (2.24)$$

Therefore, the energies of the exciton states within the exciton band are given by

$$E_{k(A)} = E_a^0 - 2 \left(\frac{N-1}{N} \right) \left[\cos \left(\frac{2\pi k}{N} \right) \right] \left(\frac{M^2}{r^3} \right) (1 - 3 \cos^2 \alpha) \quad (2.25)$$

$$E_{k(B)} = E_a^0 - 2 \left(\frac{N-1}{N} \right) \left[\cos \left(\frac{2\pi k}{N} \right) \right] \left(\frac{M^2}{r^3} \right) (1 + \cos^2 \alpha) \quad (2.26)$$

where ($k = 0, +1, -1, +2, \dots, N/2$).

Equations (2.25-26) show the interaction energy and the exciton band width, which are proportional to the square of the transition moment M for the appropriate electronic band.

The exciton bandwidths for case A and B are summarized below.

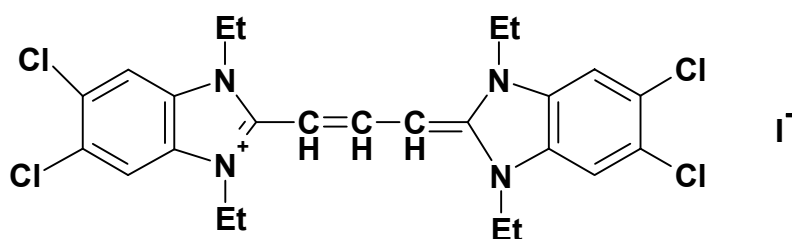
Structure	Exciton band width, 2ε
Translational chain	$4 \left(\frac{N-1}{N} \right) \left(\frac{M^2}{r^3} \right) (1 - 3 \cos^2 \alpha)$
Alternate translational chain	$4 \left(\frac{N-1}{N} \right) \left(\frac{M^2}{r^3} \right) (1 + \cos^2 \alpha)$

CHAPTER 3

SPECTROSCOPIC AND STRUCTURAL PROPERTIES OF A BENZIMIDAZOLOCARBOCYANINE DYE IN AQUEOUS SOLUTIONS

3.1 INTRODUCTION

In this chapter the spectroscopic and structural properties of the 1,1',3,3'-tetraethyl-5,5',6,6'-tetrachlorobenzimidazolocarbocyanine (TTBC) in aqueous solutions are presented.



TTBC

Figure 3.1. Chemical structure of TTBC.

Spectroscopic investigations of cyanine dyes were started in the late 1930s by Jelley and Scheibe's work on PIC J-aggregates^[4,5]. During

the last decades the photophysical properties of J-aggregates have been the subject of a large number of investigations, due to their distinctly different optical properties from those of single molecules that constitute the aggregate [38-41]. Their optical nonlinearities have attracted a lot of attention. These properties are dependent on the size of the aggregate, the molecular orientation and the transition dipole moment. These features arise from excitonic interaction between molecules, which cause delocalization of the optical excitation over the monomers of the aggregate [42-43].

Although 1,1'-diethyl-2,2'-cyanine iodide (PIC) systems have been much more investigated, the properties of TTBC are not known well, compared to PIC [44,45]. By using absorption, excitation and emission spectroscopy, the spectral properties of TTBC are investigated. In part 3.2 a computational study is provided to understand the exciton band splitting of these systems by the use of molecular exciton theory.

3.2. EXPERIMENTAL

Superradiance from aggregated benzimidazolocarbocyanines and nonlinear optical properties of TTBC draw attention of many scientists to investigate the photophysical properties. TTBC was purchased from Accurate Chemical and Scientific Co and used without further purification. Absorption spectra were recorded using Cary 5e UV-Vis-NIR spectrophotometer. The emission and excitation fluorescence spectrums were obtained by Perkin Elmer 50-B.

Figure 3.2 shows the absorption spectrum of TTBC that consists of a band at 514 nm (19455 cm^{-1}) with a shoulder at 480 nm (20833 cm^{-1}); assigned, respectively, to the 0-0 (bandwidth 791 cm^{-1}) and 1-0 (bandwidth 1600 cm^{-1}) vibronic transitions. The extinction coefficient is

calculated to be $2.0 \times 10^{-5} \text{ M}^{-1} \text{ cm}^{-1}$, which is in agreement with the literature [15]. However, the X-ray structure analysis of the TTBC single crystals indicates that the molecule is approximately planar despite extensive conjugation of π -electrons, and that the polymethine chain is twisted about 4° to minimize steric strain. In the single crystal form, the cationic TTBC molecules pack plane-to-plane and end-to-end in sheets. It was also provided that the edge of the molecular plane is 2.08 nm, and that the projected area is 0.738 nm^2 [46]. The large value of the extinction coefficient indicates an extensive conjugation of π -electrons suggesting a planar structure. As the concentration is increasing a new, narrow and intense band is observable at 587 nm (17036 cm^{-1}) called J-band (Figure 3.2).

Electrostatic forces, in addition to the hydrophobic and dispersion forces have to be considered since they play a dominant role in dye-dye interactions. In general, ionic salts, that increase the effective dielectric constant will reduce repulsion between similarly charged organic ions and thus facilitate their interaction. The opposite effect is also found with solutes that diminish this constant. Inorganic salts promote aggregation in water by increasing its effective dielectric constant. Also, pH values play an important role in aggregation. Since cyanine dyes are weak bases, H^+ ion concentration influence absorption of some dyes and the protonation products of cyanine dyes are colorless organic bis-cations. Previous studies also proved that absorption of benzimidazolocarboyanines are affected by pH variation [24, 46]. By these manners, to study the effect of ion concentration on the absorption spectrum of TTBC, NaOH is used.

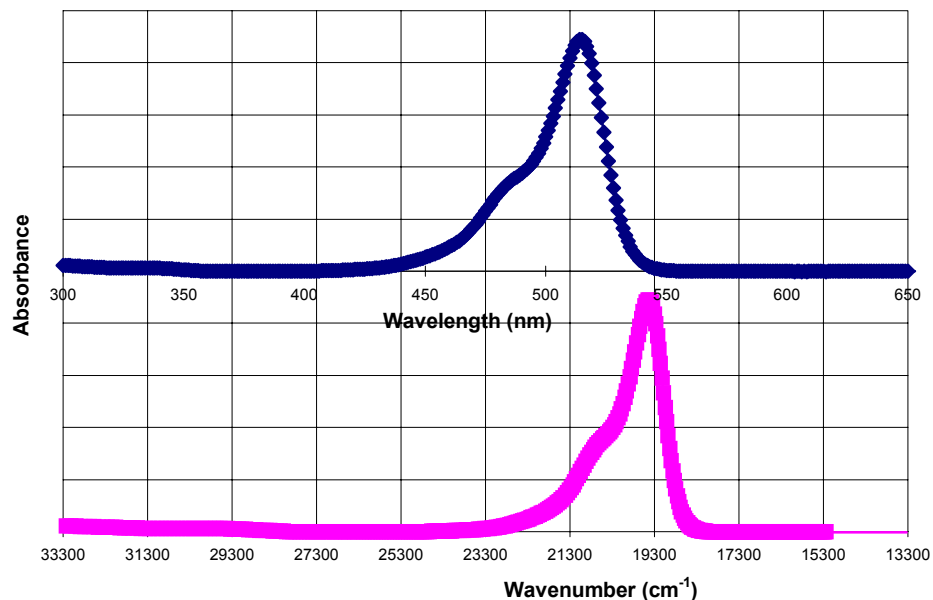


Figure 3.2. Absorption Spectrum of TTBC in methanol.

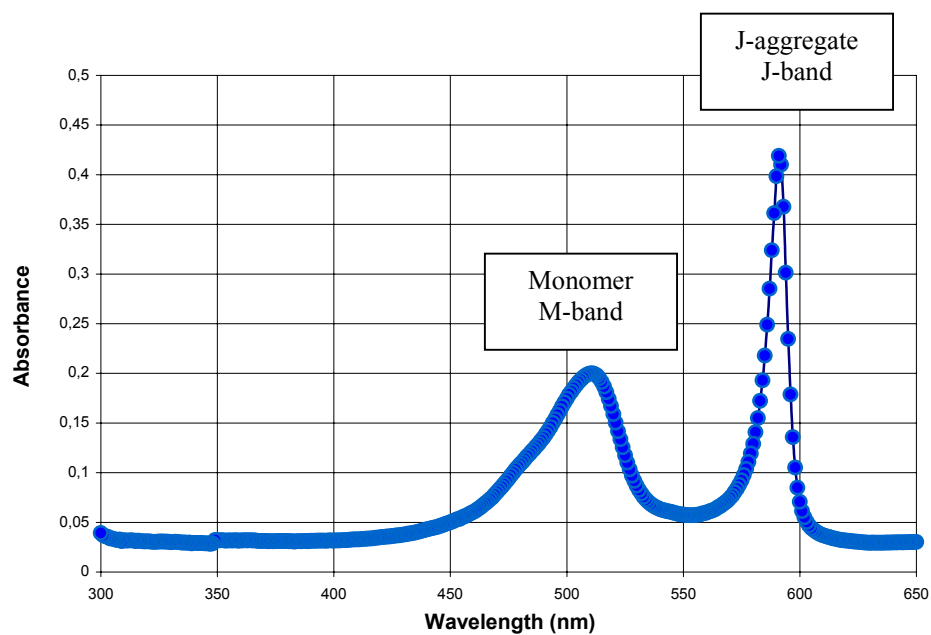


Figure 3.3. Absorption Spectrum of TTBC in aqueous solution. M-band belongs to monomer and J-band arises from J-aggregate.

As it can be seen from Figure 3.4, TTBC/NaOH aqueous solutions exhibit the characteristics of a H-band at 500 nm (20000 cm⁻¹).

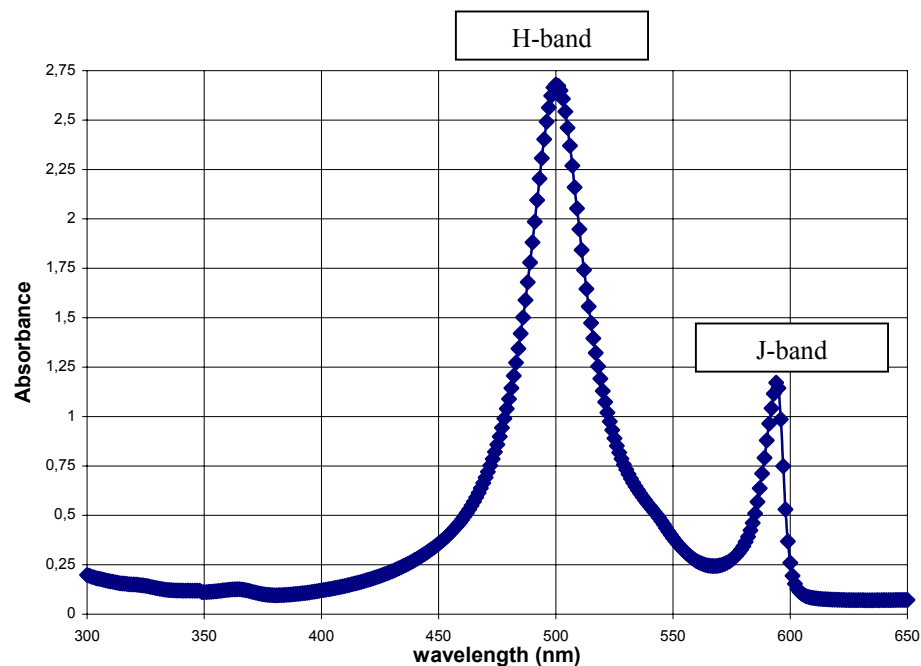


Figure 3.4. Absorption Spectrum of TTBC in aqueous solution. H-band and J-band.

The important difference between Figure 3.3 and 3.4 is H-band. Since the chemical composition of two solutions differ only in the effective NaOH concentration, we can say that the ion concentration of the medium has a direct effect on the structural properties of aggregates, which are resulting in transformation of monomer to H-aggregate. The occurrence or disappearances of transitions are strictly dependent on the physical properties of aggregates. So to have a better understanding of the properties of aggregates, ion and dye concentration dependency of absorption spectrum has to be studied.

3.2.1. Effect of NaOH Concentration on Aggregation

Samples were prepared by mixing TTBC/MeOH solutions with different concentrations of NaOH solutions ranging from 1.00M to 0.01 M in 1 to 4-volume ratio. Figure 3.5 shows the effect of ion concentration on the exciton bands. When the ion concentration is 1.00 M NaOH, the

spectrum is dominated by a broad J-band, which indicates the existences of different types of aggregates are present in medium. This suggests variable transition dipole moment orientations resulting in a broader exciton band. By decreasing NaOH concentration, H-band intensity increases and both J- and H-band became narrower.

The important outcome of this spectrum is the transfer of the intensity from the H-band to the J-band by increasing the NaOH concentration. It suggests a change of the orientation of the transition moments, intermolecular distance, mutual intermolecular orientation. All of these effects may manifest themselves on the absorption spectra of the aggregate.

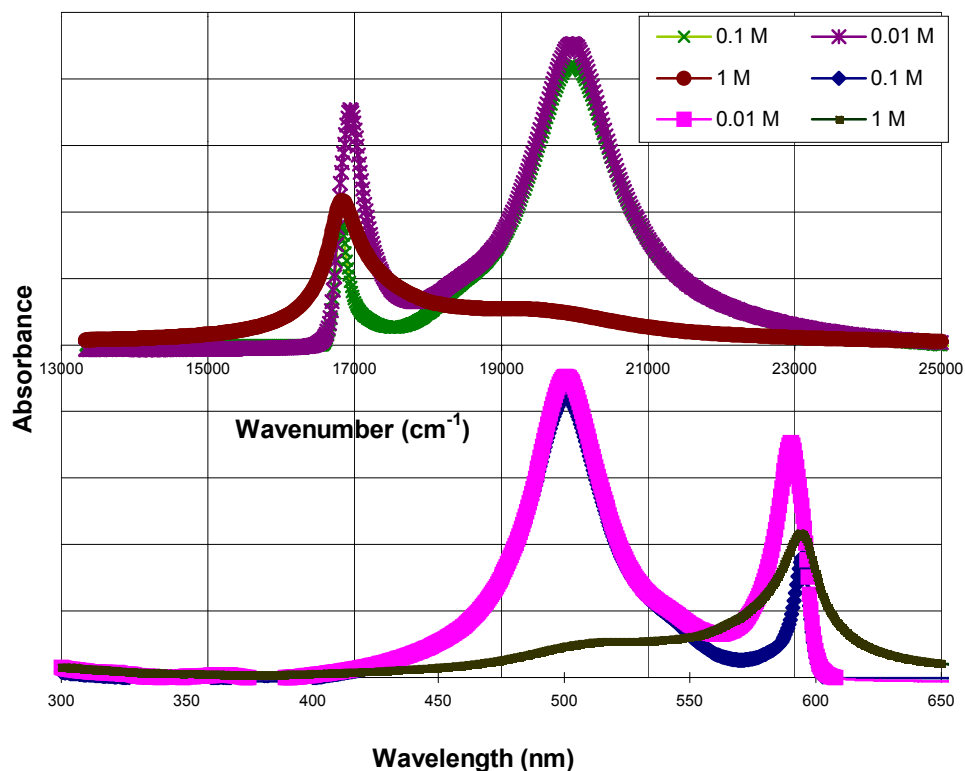


Figure 3.5. Absorption spectra of TTBC/NaOH aqueous solutions for different NaOH concentrations. [TTBC] = 1×10^{-4} M in methanol.

3.2.2. Effect of TTBC Concentration on Aggregation

The second step is to understand the effect of dye concentration on the aggregation, since the position, intensity and shape of the spectrum primarily depends on the concentration of dye. The samples are prepared by the same procedure that was described in the previous section. Dye concentration varying in the range of $1.0\text{-to-}9.0 \times 10^{-4}$ M (Figure 3.6).

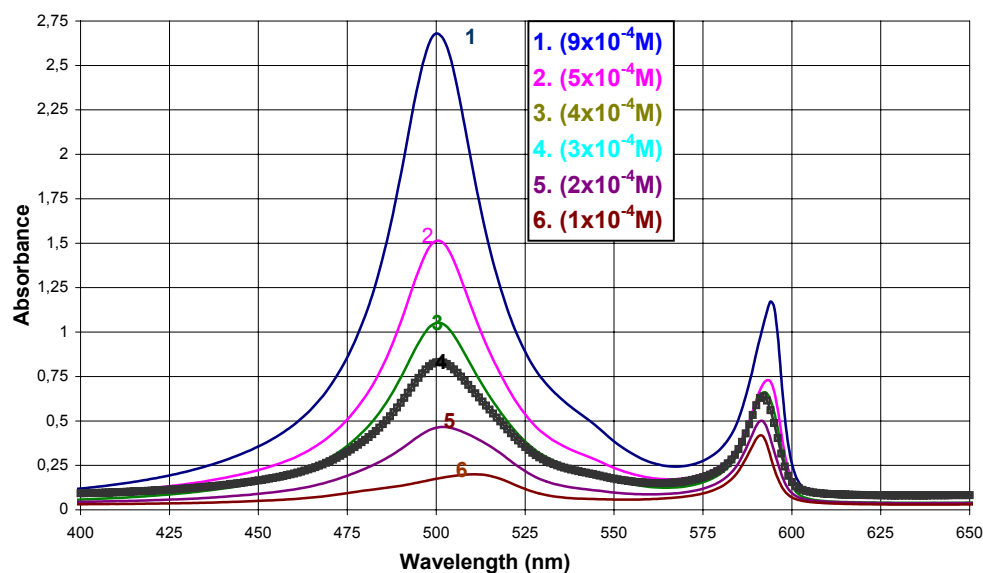


Figure 3.6. The change of the absorption spectrum of TTBC/NaOH aqueous solutions for different TTBC concentrations. $[\text{NaOH}] = 0.01\text{M}$.

When the TTBC concentration is high, the H-band dominates over the J-band, when the concentration is lowered there is a substantial shift to the J-band. The second important result is, that as the dye concentration decreases, the J-band shifts from 590 nm to 594nm, while the H-band disappears and the M-band reappears. (Figure 3.7 and Figure 3.8).

By varying the concentration we are able to control the electronic structure of the exciton band that is the shift from the H-band to the J-band. Therefore, we propose that the primary effect causing the change of the spectrum should arise from the structural change of the aggregate. If

one can control the electronic/structural properties, then the control of the optical properties is feasible.

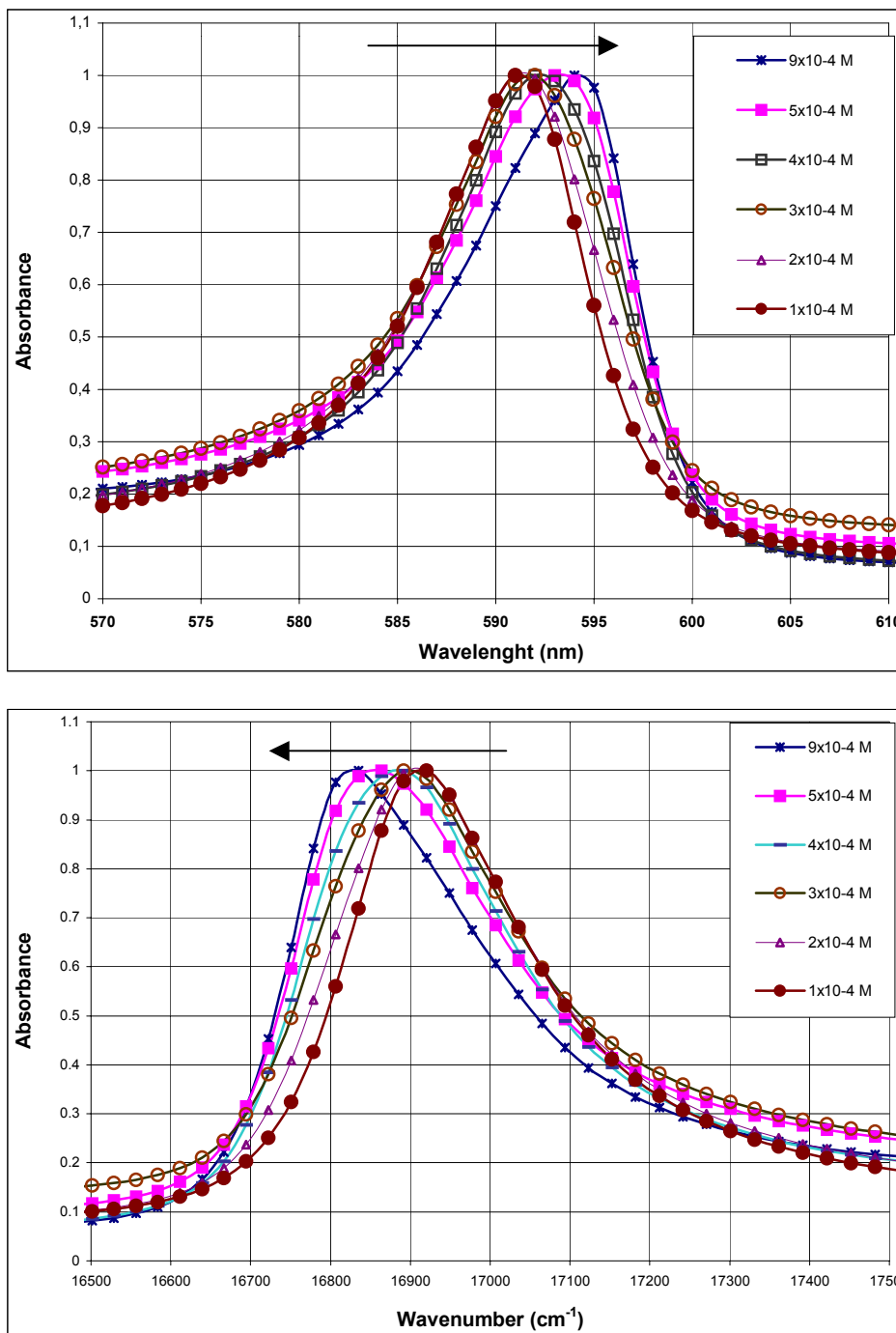


Figure 3.7. Normalized absorption spectra of TTBC in aqueous solution, $[\text{NaOH}] = 0.01 \text{ M}$.

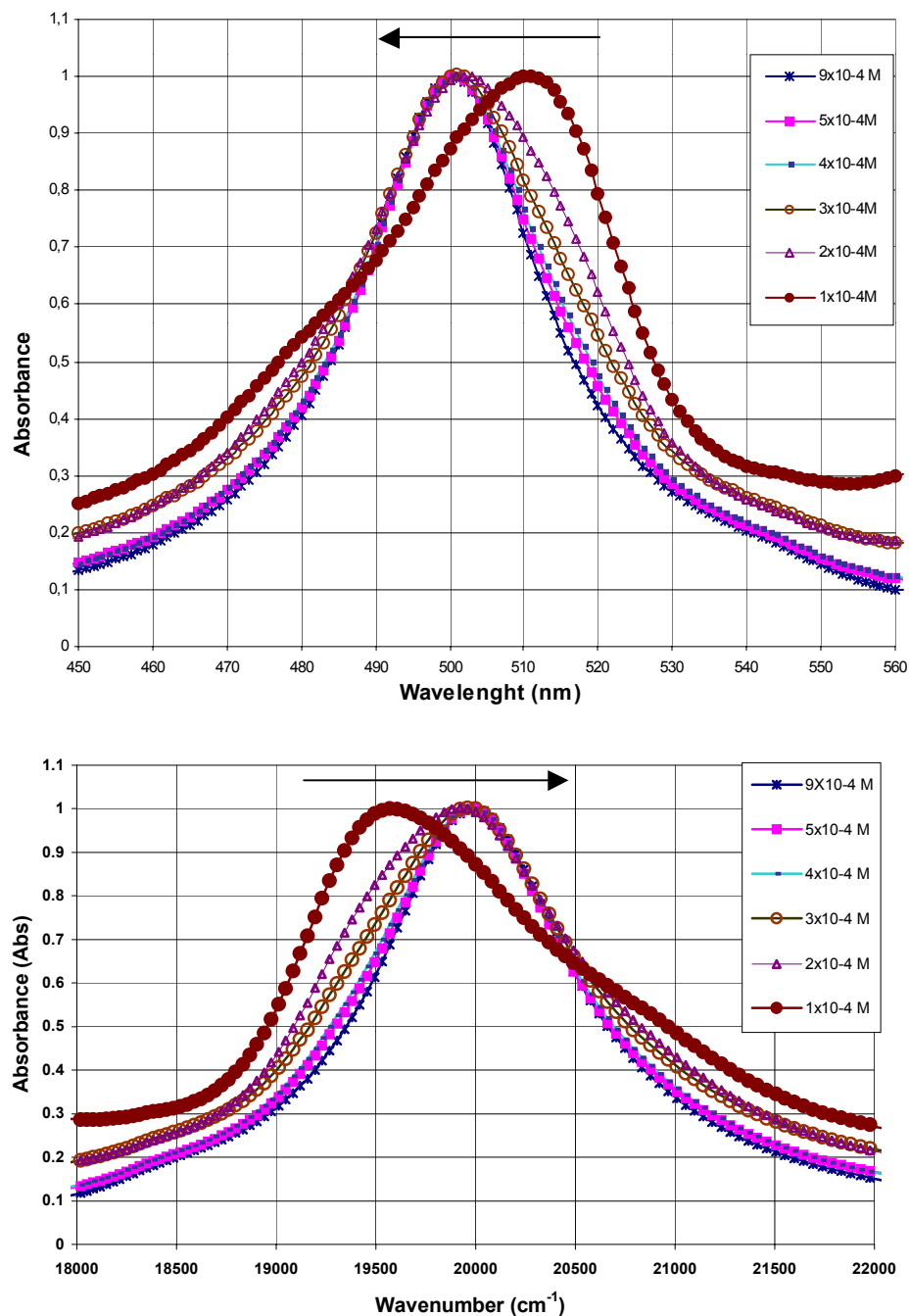


Figure 3.8. Normalized absorption spectra of TTBC in aqueous solution, $[\text{NaOH}] = 0.01 \text{ M}$.

As we look deeper to experimental study, we see that the absorption spectrum of TTBC solutions have a shoulder on J-band. The nonlinear curve fitting of this part of the spectrum using Voigt (Area,

Gaussian/ Lorentzian Widths) method two distinct bands are found. These bands are assumed to be oriented due to the coupling of the aggregate chains. (Figure 3.9)

By concentration increase it was seen that the band, due to the coupling, is red-shifted. The relative intensities have a decreasing pattern with respect to concentration, by that way figure might be misleading.

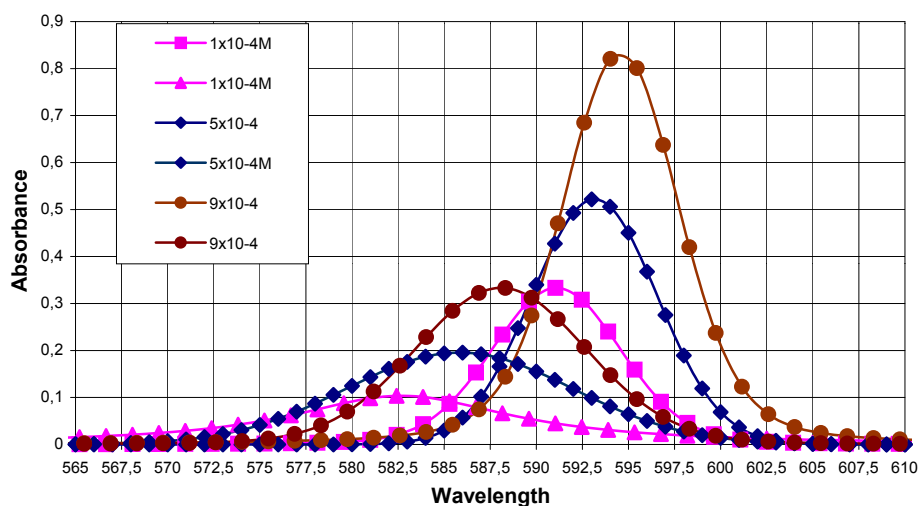


Figure 3.9. The change of the absorption spectrum of TTBC/NaOH aqueous solutions for different TTBC concentrations. [NaOH] = 0.01M.

The relative intensities and positions of bands with respect to concentration are:

Concentration	Band position	Relative Intensity
9×10^{-4} M	588 nm	3.04
9×10^{-4} M	594 nm	5.53
5×10^{-4} M	585 nm	4.11
5×10^{-4} M	593 nm	6.08
1×10^{-4} M	582 nm	16.47
1×10^{-4} M	591 nm	22.42

3.2.3. Fluorescence Emission and Excitation Spectroscopy

Figure 3.10 shows the fluorescence spectrum of TTBC in methanol, excited at ca. 450nm. The fluorescence has a maximum at ca. 528 nm, and a shoulder at ca. 560 nm^[15].

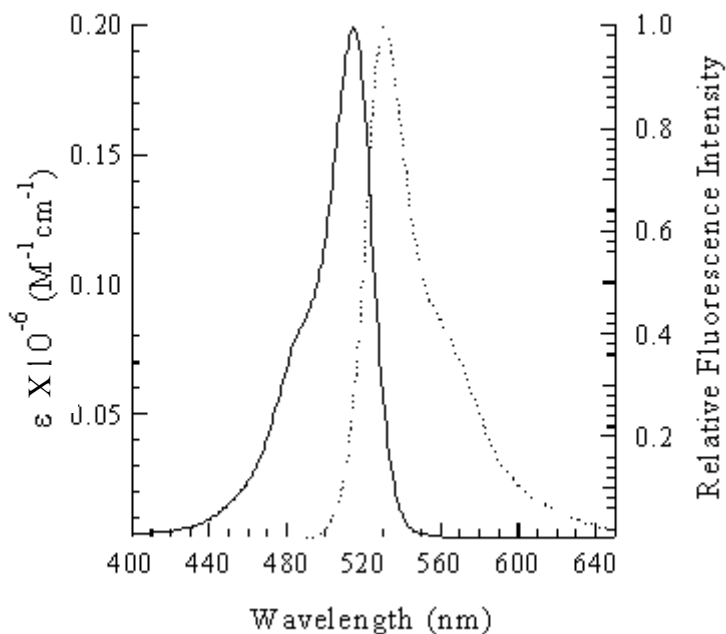


Figure 3.10. Absorption and fluorescence spectra of TTBC in methanol at room temperature. [TTBC = 1×10^{-5} M].

Figure 3.11 represents the fluorescence emission and excitation spectrum of TTBC in aqueous solution at room temperature.

The fluorescence spectrum reveals two important features: First, there is a split band structure of the excitation spectrum, which is the same as the absorption spectrum. This proves that the solution consists of two different structural units within the molecular aggregate, first an H-aggregate having a fluorescence excitation maximum at 500 nm, and second a J-aggregate having a fluorescence excitation maximum at 596

nm. The excitation spectrum is detected at 620 nm, which is in the fluorescence band of the aggregate emission.

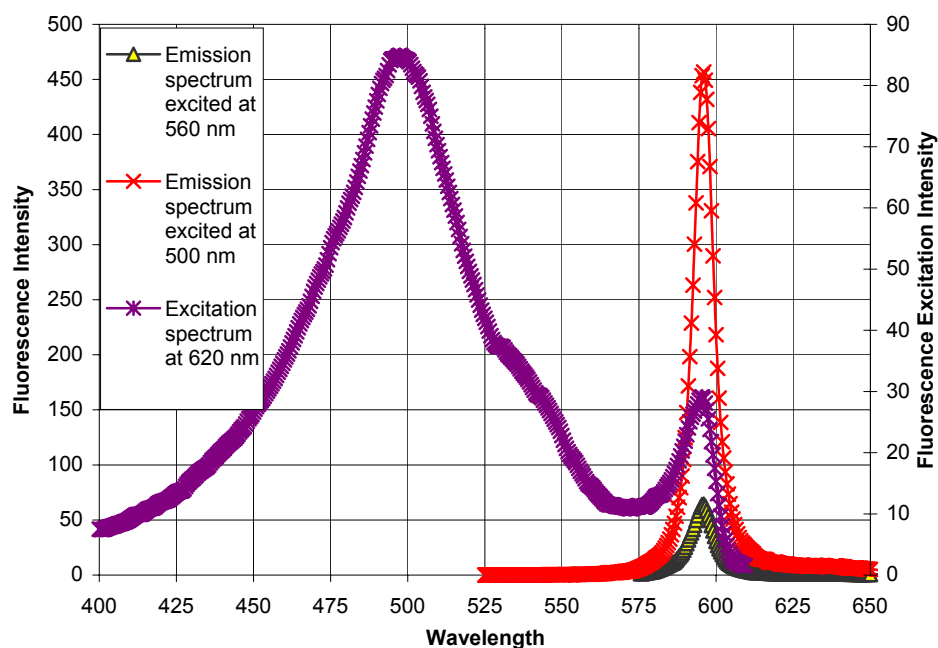


Figure 3.11. Fluorescence spectrum of TTBC/NaOH aqueous solution.

Second, both bands are coupled to each other that is an indication of an energy transfer from H-band to J-band, because both excitations result in one emission band at 596 nm. The collective response of the two structural units results in an increase of the intensity of the emission spectrum excited at 500nm, which is more intense than the emission spectrum excited at 560 nm. The relaxation of the upper molecular exciton band to the lower band results in an increase in the intensity.

CHAPTER 4

COMPUTATIONAL and THEORETICAL WORK

4.1. INTRODUCTION

Many theoretical studies were performed on the aggregates of cyanine dyes. Dimerization, intermolecular coupling, molecular orbital calculations were studied to simulate the optical properties of the collective response of cyanine dyes ^[22,48]. Among the cyanine dyes, PIC was the most extensively studied. The coupling and the splitting of an exciton band are often studied in the literature ^[6,20-22]. The splitting of bands in the electronic or vibrational spectra of crystals due to the presence of more than one (interacting) equivalent molecular entity in the unit cell is known as Davydov splitting (factor-group splitting). But the characteristic of the Davydov splitting is the symmetrical shift of the exciton bands with respect to the monomer band. The symmetrical splitting of the exciton band is thought to be influenced by many factors, which are studied experimentally and theoretically over years ^[47]. The interesting feature of our study is the asymmetrical splitting of the molecular exciton band with respect to the monomer band. No theoretical or computational study has been presented so far in the literature for such an experimental data on TTBC. This novel approach to this experimental

data aims to develop a theoretical explanation to enhance our understanding of structural effects on optical properties and to explain the asymmetrical splitting based on structural properties of the aggregates.

To present a theoretical work, we first need to determine the first order exciton state energy (E) and interaction energy (ε) by use of the molecular exciton theory.

The first part of the theoretical work aim to explain the aggregate behavior of single chains constituting J- and H-bands. The geometry on Figure 2.4 corresponds to J-aggregate ($0^0 \leq \alpha \leq 54.6^0$) and H-aggregates ($90^0 \geq \alpha \geq 54.6^0$). For these cases where $\alpha = 0$ and $\pi/2$, the transition energies and the transition moments for the m^{th} exciton state are ^[33,47,48]:

$$E_k = E_0 + 2\varepsilon \cos\left(\frac{\pi k}{N+1}\right) \quad (4.1)$$

$$M = M_{mon} \sqrt{\left(\frac{2}{N+1}\right) \frac{1-(-1)^k}{2}} \cot\left(\frac{\pi k}{2(N+1)}\right) \text{ where } k=1,2,3,\dots,N \quad (4.2)$$

where N is the number of molecules forming the aggregate and ε_{nm} is the interaction energy between molecules n and m , which is assumed to be of dipolar origin.

If we modify the Equation 2.18 to apply in this case,

$$\varepsilon = \frac{|M|^2}{5.04R^3} (1 - 3 \cos^2 \alpha) \quad (4.3)$$

where ξ_0 is the permittivity of the vacuum, η is the refractive index of the medium, M is the transition dipole moment of the monomer, R is the distance between nearest neighbors in the aggregate, and α is the angle between monomer transition vector in the aggregate (monomer is considered to be in a solution). For a "linear" aggregate $\alpha=0$; for an "alternate" aggregate, $\alpha \neq 0$. For a J-aggregate the exciton coupling energy

ϵ is negative, which leads to red-shifts in the spectrum relative to the monomer. By contrast, ϵ is positive for H-aggregates, causing blue shifts in the spectrum. For the calculations, by using the literature data, the transition dipole moment was taken as 10 Debye ($1\text{D} = 1 \times 10^{-18} \text{esu cm}$)^[49].

4.2.1. Interaction Energy and Size Dependency of Absorption Spectrum for J-band and H-band for Single Chain

Equation 4.1 shows that the interaction energy is equal to twice of the band splitting between monomer band and J-band, when N is large. Therefore the interaction energy, ϵ is about -1300 cm^{-1} . By using equations 4.2 and 4.3, the interaction energy was found to be between 1250 cm^{-1} to 1350 cm^{-1} , and the number of molecules to form J-aggregate should be equal or bigger than ten. (Figure 4.1)

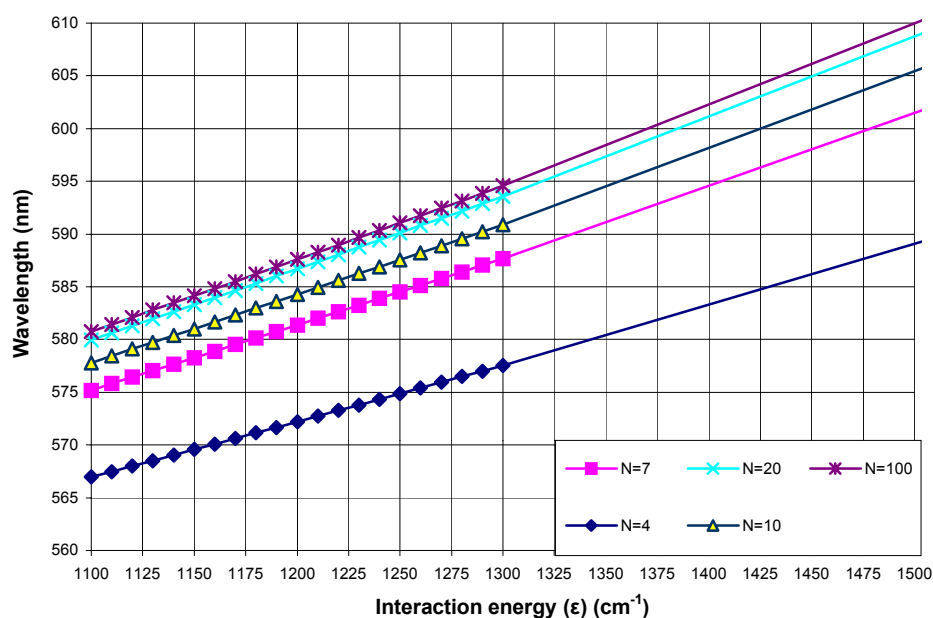


Figure 4.1. The J-band absorption maximum as a function of interaction energy (ϵ), and number of molecules forming the aggregate (N).

By the same manner, the interaction energy for the H-aggregate was found to be approximately 325 cm^{-1} , when the position of H-band is taken at 500 nm . By using the same calculation procedure as in the case of

J-band, interaction energy (ϵ) was found to be between 280 cm^{-1} to 320 cm^{-1} , and N was found to be bigger than 7.

The size of the aggregate, N , is a determining factor for the band position of absorption spectrum. But, the spectrum saturates for bigger aggregates whereas $N \geq 15$. It suggests that the collective coupling of the transition moments tend to be localized on a definite structural size^[18,41]

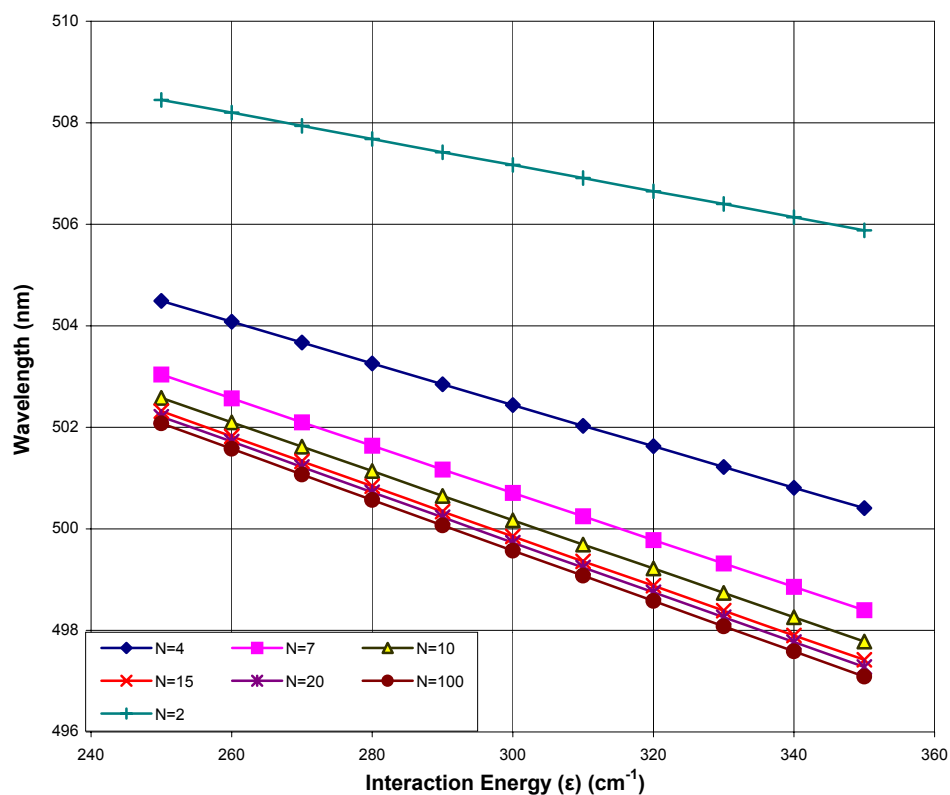


Figure 4.2. The H-band absorption maximum as a function of interaction energy (ϵ), and number of molecules forming the aggregate (N)

4.2.2. Molecular Orientation and Intermolecular Distance Dependency of Absorption Spectrum for J-band and H-band for Single Chain

The Equation 4.3 uses three important parameters to calculate the interaction energy: the size of transition dipole moment, the mutual molecular orientation, that the angle between the aggregate axis and the molecule, and on the intermolecular distance. To estimate the interaction energy by using these values, a number of iterating calculations have to be carried on. Such specific molecular orientations, α , and intermolecular distances, R , have to be chosen to satisfy the experimental values.

The interaction energy (ϵ), for J-aggregate was estimated to be between 1250 cm^{-1} and 1350 cm^{-1} . The intermolecular distance is estimated to be between 4.5 to 9.5 \AA . The angle between molecules is estimated to be between 50° and 10° from the Figure 4.3. The steric factors are also taken into account.

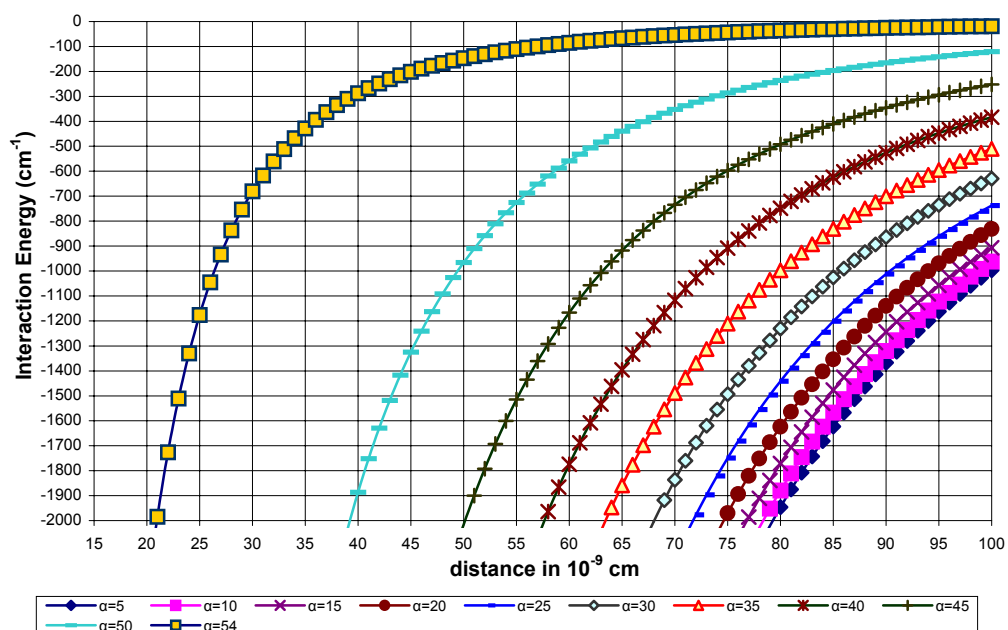


Figure 4.3. Molecular orientation and intermolecular distance dependence of absorption spectrum for the J-band.

The same calculation procedure for H-band, where the interaction energy is between 280 cm^{-1} and 320 cm^{-1} carried out to estimate the distance between molecules forming the aggregate to be between 2,8 and 9.5 \AA . The angle between molecules is estimated to be between 55° and 70° . (Figure 4.4)

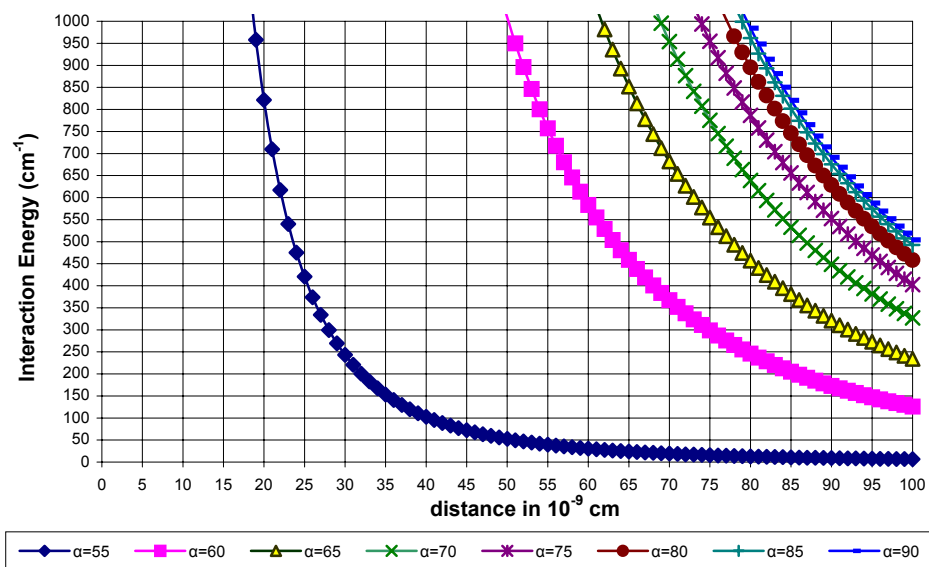


Figure 4.4. Molecular orientation and intermolecular distance dependence of absorption spectrum for the H-band.

4.3. Single Chain Dependency on Molecular Structure

This part aims to explain the absorption spectrum by considering the splitting, which is due to the structural changes in the aggregate chain.

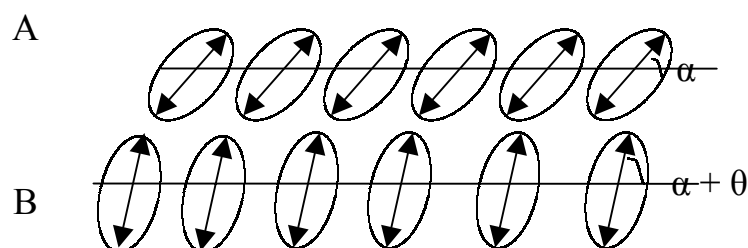


Figure 4.5. A representative scheme for a J-aggregate (A) and a H-aggregate (B)

By using the relationship between the interaction energy and intramolecular distance, we can write such an equation to cover the effect of transformation from J-band to H-band:

$$\varepsilon_{\text{H-band}} = \frac{|M|^2}{4\pi\xi_0\eta^2R^3} [1 - 3\cos^2(\alpha + \theta)] \quad (4.4)$$

where, θ represents the angle shift to change the orientation from an J-aggregate to an H-aggregate

$$\theta = \cos^{-1} \left[\frac{1-R'}{3} + R' \cos^2 \alpha \right]^{\frac{1}{2}} - \alpha \quad (4.5)$$

$$\text{if } R' = \left(\frac{\varepsilon_H}{\varepsilon_j} \right) / \left(\frac{r_H}{r_j} \right)^3 \quad (4.6)$$

Figure 4.6 shows the change of molecular orientation according to the Equation 4.5. Experimental results yield that, R' is changing from 0.5 to 0.12. We may calculate the intermolecular distance and α and θ values from Figure 4.5 It manifests that α varies between 10° and 50° , θ values must change from 60° to 5° .

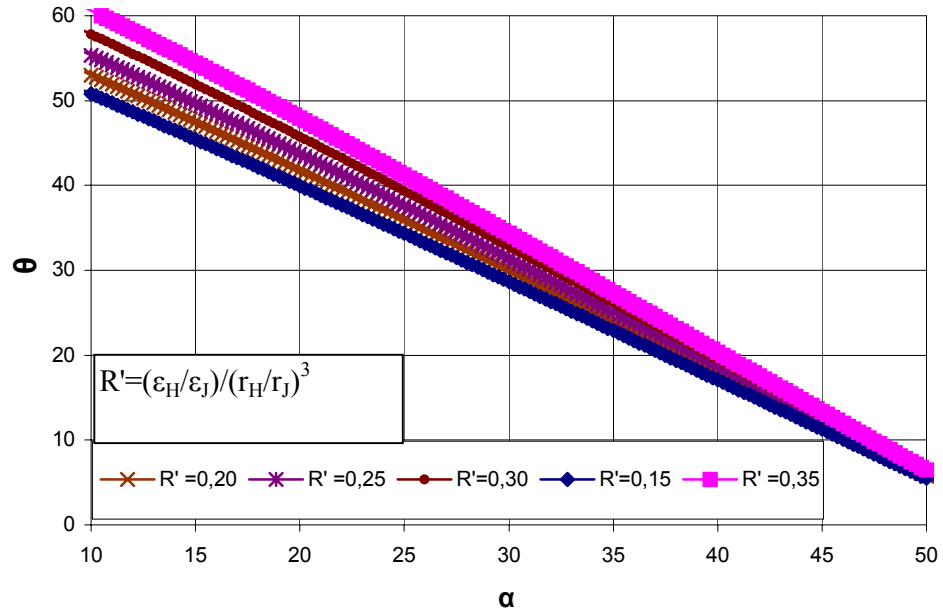


Figure 4.6. The Change of molecular orientation according to Equation 4.5.

Figure 4.7 and 4.8 show the change of the intermolecular distance with respect to molecular orientation as a function of interaction energy. The intermolecular distance between the molecules forming J-aggregate and H-aggregate was respectively obtained to be 9.2 Å to 4.4 Å for J-aggregate and 2.7 Å to 9.4 Å .

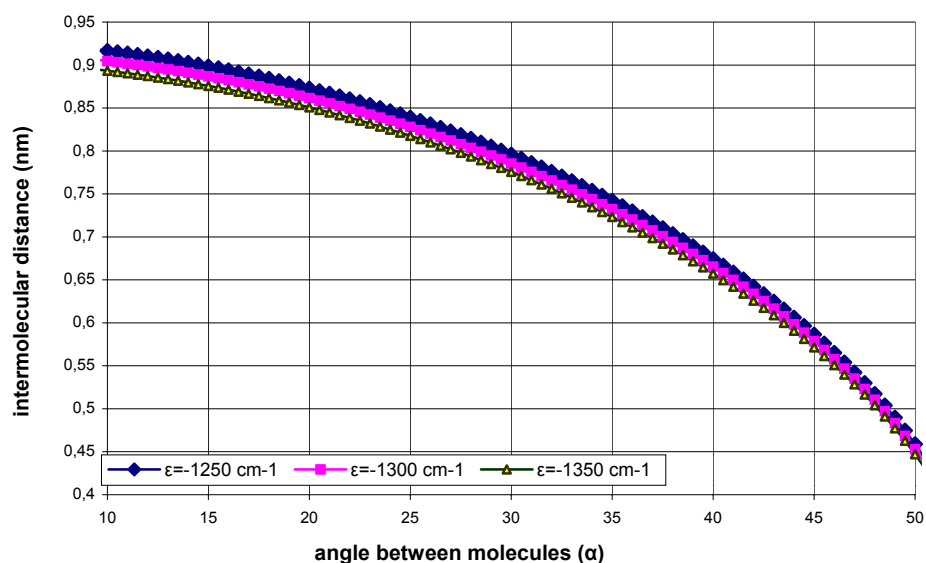


Figure 4.7. Change of intermolecular distance with respect to molecular orientation as a function of interaction energy for the J-band.

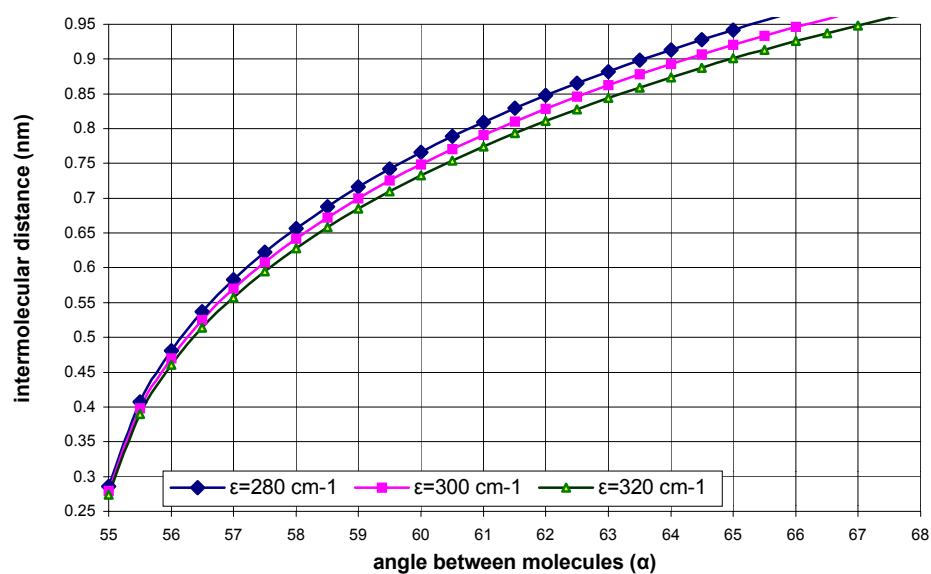


Figure 4.8. Change of intermolecular distance with respect to molecular orientation as a function of interaction energy for H-band.

Until now, a single J-aggregate and/or H-aggregate cases were studied. But our experiments indicate that both structural units, J- and H-aggregate contribute to the spectral features, so the models presented are, inefficient to describe the absorption spectra.(Figure 3.6) We propose a novel method to explain the asymmetrical splitting of the exciton band with respect to monomer band. This model suggests the coupling of molecules residing at the ends of the aggregate chains. The molecules residing at the end are in a close proximity to interact. The steric contributions are also taken into account for the calculations.

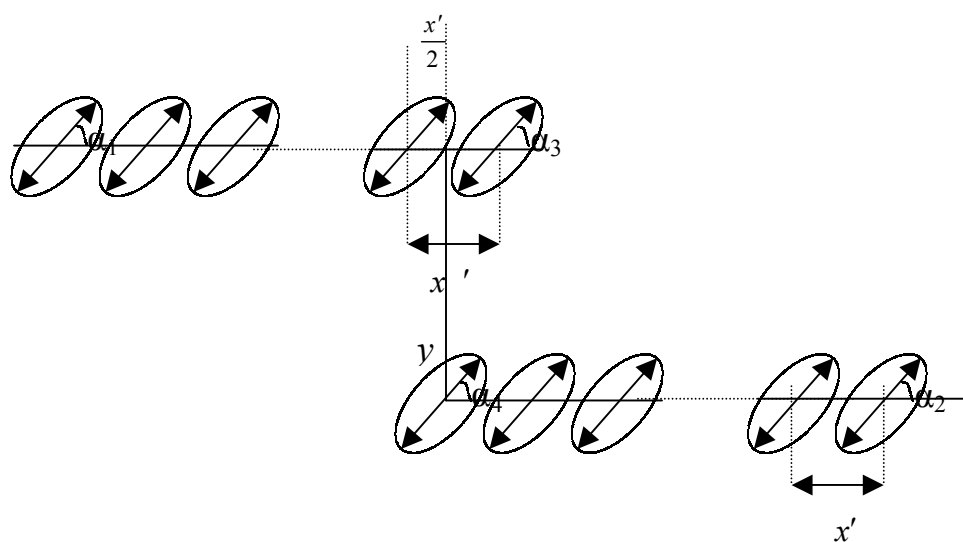


Figure 4.9. The geometry of the novel method proposed for the interacting chains.

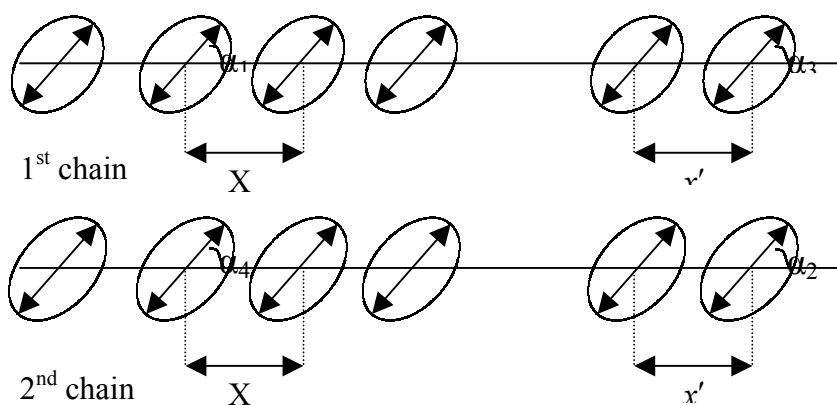


Figure 4.10. The interaction geometry for the chains.

By considering the geometries in Figure 4.8 and 4.9, we obtain:

$$\begin{aligned}\varepsilon_1 &= \frac{|M|^2}{5.04x^3}(1-3\cos^2\alpha_1), \quad \varepsilon_2 = \frac{|M|^2}{5.04x^3}(1-3\cos^2\alpha_2) \\ \varepsilon_3 &= \frac{|M|^2}{5.04x'^3}(1-3\cos^2\alpha_3), \quad \varepsilon_4 = \frac{|M|^2}{5.04x'^3}(1-3\cos^2\alpha_4)\end{aligned}\quad (4.7)$$

$$\begin{aligned}\varepsilon_{13} &= \frac{|M|^2}{5.04x^3}(\cos\alpha_1\cos\alpha_3 + \sin\alpha_1\sin\alpha_3 - 3\cos\alpha_1\cos\alpha_3) \\ \varepsilon_{24} &= \frac{|M|^2}{5.04x^3}(\cos\alpha_2\cos\alpha_4 + \sin\alpha_2\sin\alpha_4 - 3\cos\alpha_2\cos\alpha_4)\end{aligned}\quad (4.8)$$

We define the interaction between the chains through the molecules at the end

$$\begin{aligned}\varepsilon_{34} &= \frac{|M|^2}{5.04(yx)^3}[(\cos\alpha_3\cos\alpha_4 + \sin\alpha_3\sin\alpha_4)] \\ &- 3\frac{|M|^2}{5.04(yx)^5}\left[\left(\cos\alpha_3\frac{x'}{2} - \sin\alpha_3y\right)\left(\cos\alpha_4\frac{x'}{2} - \sin\alpha_4y\right)\right]\end{aligned}\quad (4.9)$$

$$\text{where, } (yx) = \left[\left(\frac{x'}{2}\right)^2 + y^2\right]^{\frac{1}{2}}$$

The model developed depends on many variables: the molecular orientations $[(\alpha_{1,2}), \alpha_{3,4} = \theta_{1,2} + \alpha_{1,2}]$, intermolecular distances (x, y) , transition dipole moment (M^2) and the size of the aggregate $(N_{c1}$ and $N_{c2})$. The chain properties are taken as independent of each other. A Fortran program was written by Prof. Gulen is used to study the effects of these variables on the interaction of two aggregate chains related to the absorption spectra.

The outcome of the investigation on the variables affecting the interaction will be discussed as follows:

a) The size effect: Equations 4.3–4.5 clearly states that the interaction energy, the transition moment and the molecular exciton state energy are all dependent on size of the aggregate.

The predictions of the model for the different size of the aggregate chain can be seen from Figure 4.10. For this calculation the total number of molecules forming the aggregate chains are fixed to 48. According to the model as the size of the aggregate chain is increasing, for the J-aggregate chain the band position shifts to higher wavelengths (lower energy) and for the H-aggregate the band position shifts to smaller wavelengths and both band intensities increase, which means delocalization of the molecular excited levels are more feasible at higher numbers molecules forming the aggregate chain.

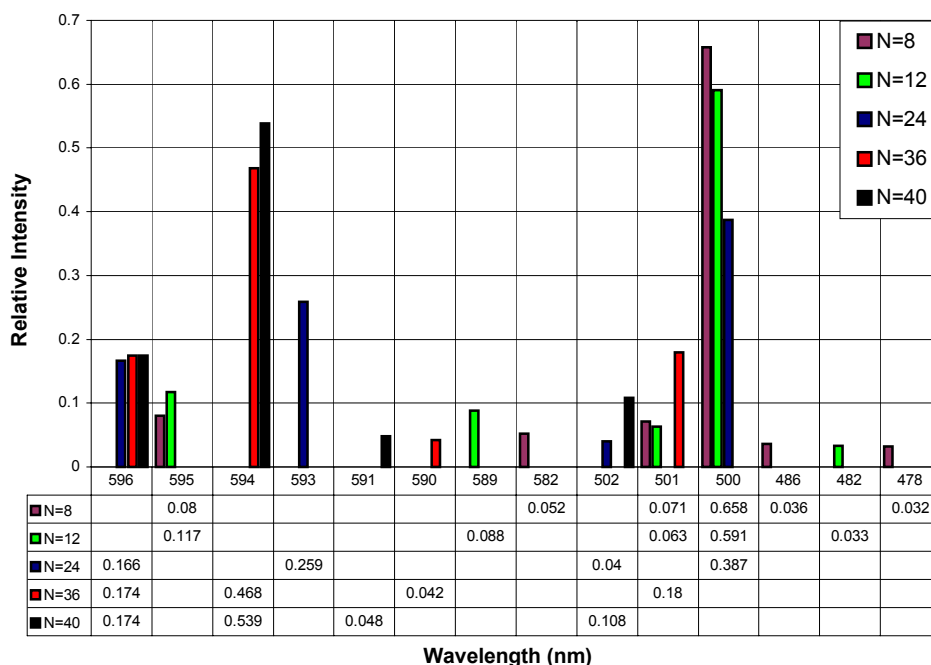


Figure 4.11. The change of the absorption spectra with respect to the number of molecules forming the aggregate.

b) The effect of molecular orientation: In section 1.2 and 2.4, it was stated when the angle between the molecules and the aggregate axis, α , has the range $0^{\circ} \leq \alpha \leq 54.6^{\circ}$; the J-aggregate characteristics appear in the spectrum. The chain has the H-aggregate characteristics for the range of $54.6^{\circ} \leq \alpha \leq 90^{\circ}$. As α is decreasing J-band is red-shifted, and H-aggregate is blue-shifted.

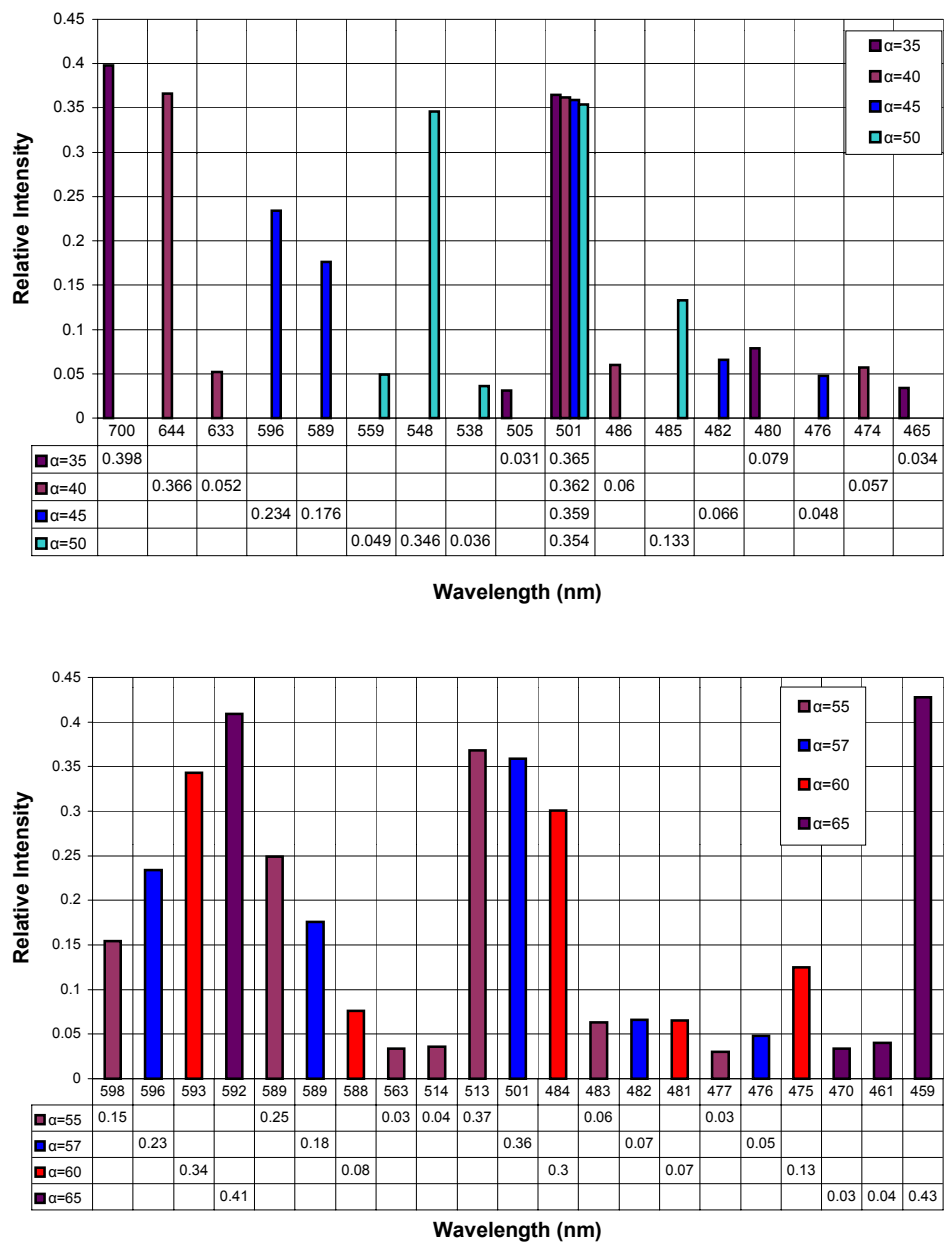


Figure 4.12. The change of the absorption spectra with respect to the mutual orientation of the molecules forming J- and H-aggregate

By calculations it was seen that the change of the angle between molecules constituting aggregate chains and the intensity of the bands have a direct relation. For J-aggregate by the increase of the angle between molecules the intensity of the lower exciton band is transferred to the higher exciton band. For H aggregate, by increase the same pattern is observable.

c) The intermolecular distances: It is evident that the interaction energy between molecules strongly depends on the distance (expressed as X in our model, in general R) between molecules. As the separation between molecules increases, the interaction between molecules will decrease with the one-third power of the distance (see Equation 4.2, 4 and 8) (Figure 4.13).

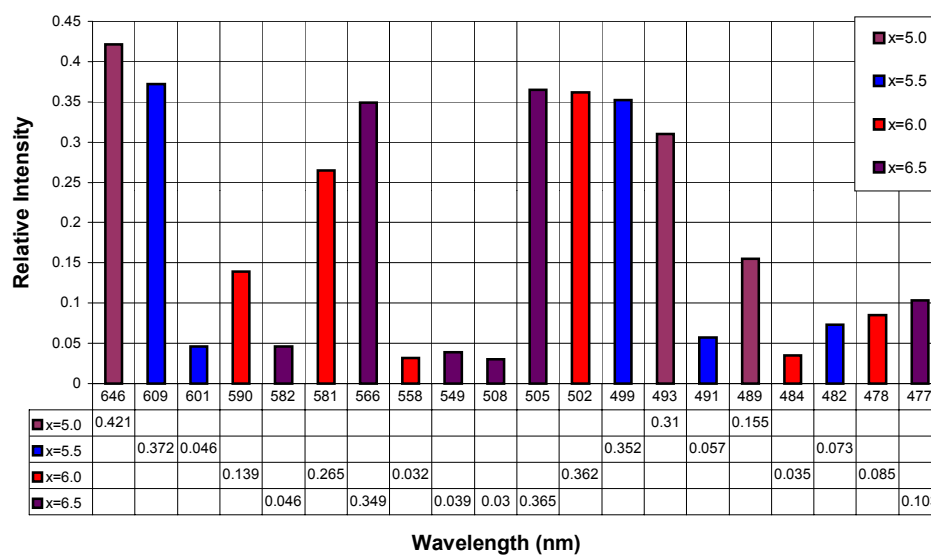


Figure 4.13. The change of the absorption spectra with respect to the distance between the molecules.

The strength of the coupling of the chains depends on the distance. As the aggregate chains become closer, the splitting of the bands between

chains increases (represented as y in our model). When the distance between the interacting chains is between 6.5 Å and 5.0 Å the model predicts some transitions within the J-band. When the distance is out of the abovementioned range, the model predicts single transitions in the bands. The changes of the distances are compensated by the mutual orientation of the molecules to optimize the interaction.

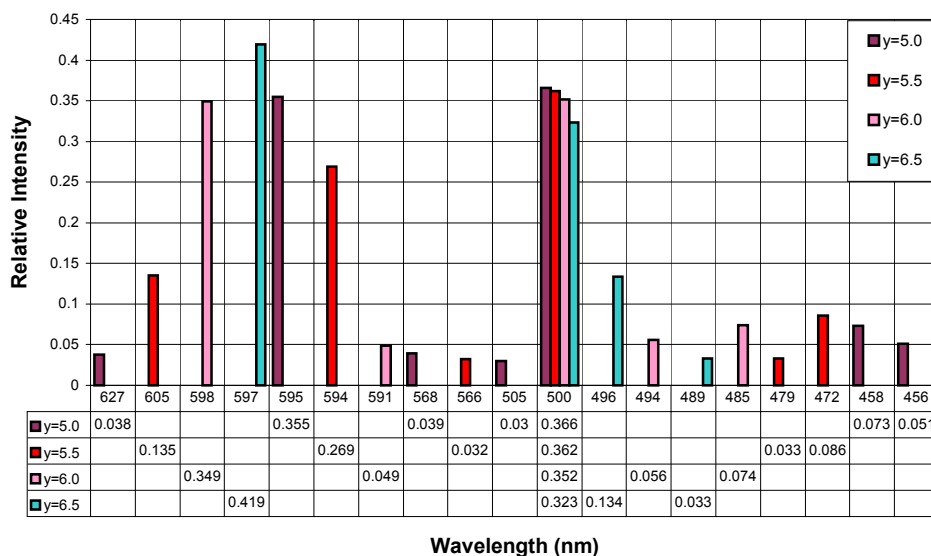


Figure 4.14. The change of the absorption spectra with respect to the distance between interacting molecular aggregate chains.

CHAPTER 5

CONCLUSION

The spectral and structural properties of J-aggregates of 1,1',3,3'-tetraethyl-5,5',6,6'-tetra-chlorobenzimidazolocarboyanine (TTBC) are investigated. J-aggregates formed by TTBC were presented by structural parameters such as the transition dipole moment, the intermolecular distance and mutual intermolecular orientation.

The observed asymmetrical splitting of the exciton band is found to be dependent on dye and NaOH concentration. Fluorescence emission and excitation spectroscopy studies proved that the solution consists of two different structural units within the molecular aggregate in which the exciton bands are coupled with each other. The experimental data proved that a transfer occurs excitation energy between two aggregate chains.

A computational study is provided to explain the exciton band splitting. The intermolecular distance, the mutual orientation of molecules and the size of the aggregates are found to be influencing the absorption spectrum. All of these variables are set within a range of values to satisfy the experimental findings. A molecular aggregate chain orientation model

is proposed and used to examine the asymmetrical splitting of the molecular exciton bands. According to the model proposed, the coupling of the two aggregate chains is proved.

REFERENCES

- [1] Feldmann J., Peter G., Gobel E. O., Dawson P., Moore K., Foxon C. and Elliott R. J., "Linewidth dependence of radiative exciton lifetimes in quantum wells". *Phys. Rev. Lett.*, **59**, (1987) 2337-2340.
- [2] Terpstra J., Fidler H. and Wiersma D. A., "A nonlinear optical study of Frenkel excitons in Langmuir-Blodgett films". *Chemical Physics Letters*, **179 (4)**, (1991) 349-354.
- [3] Fidler H., Terpstra J. and Wiersma D.A., "Dynamics of Frenkel excitons in disordered molecular aggregates". *Journal of Chemical Physics*, **94 (10)**, (1991) 6895-6907.
- [4] Scheibe G., Über die Veränderlichkeit der Absorptionsspektren in Lösungen und die Nebenvalenzen als ihre Ursache. *Angew. Chem.*, **50**, (1937) 211-219.
- [5] Jelley E. E., Molecular, "Nematic and Crystal States of Pseudoisocyanine Chloride (PIC)". *Nature*, **139**, (1937) 631-632.

- [6] Van der Auweraer M. and Scheblykin I., "One-dimensional J aggregates: Dependence of the Properties of the Exciton Band on the Model of the Intermolecular Coupling". *Chemical Physics*, **275**, (2002) 285-306.
- [7] Knapp E. W., "Lineshapes of Molecular Aggregates, Exchange Narrowing and Intersite Correlation". *Chemical Physics*, **85 (1)**, (1984) 73-82.
- [8] Moll J., Daehne S., Durrant J.R. and Wiersma D.A., "Optical Dynamics of Excitons in J-aggregates of a Carbocyanine Dyes". *J. Chem. Phys.*, **102 (16)**, (1995) 6362-6370.
- [9] Frenkel J., "On the Transformation of Light into Heat in Solids.2". *Phys. Rev.*, **37**, (1931) 17-44.
- [10] Wannier G.H., "The Structure of Electronic Excitation Levels in Insulating Crystals". *Phys. Rev.*, **52**, (1937) 191-197.
- [11] Mott N F and Littleton M J, "Conduction in polar crystals: Electrolytic conduction in solid salts". *Trans Faraday Soc*, **34**, (1938) 485-489.
- [12] Knox R.S., "Theory of Excitons". Acad. Press., New York (1963)
- [13] Herz A., "Dye-dye interactions of Cyanines in Solution and at AgBr Surfaces, Photographic Science and Engineering". *Photographic Science and Engineering*, **18 (3)**, (1974) 323-335.
- [14] Knapp E. W. and Fischer S. F., "Exchange Narrowing of Correlated Inhomogeneities. The Dimer Lineshape". *Chemical Physics Letters*, **103 (6)**, (1984) 479-483.

- [15] Ozcelik S., “Steady State and Picosecond Time-Resolved Photophysics of a Benzimidazolocarboyanine Dye”. *Journal of Luminescence*, **96 (2-4)**, (2002) 141-148.
- [16] Knoester J., “Nonlinear Optical Line Shapes of Disordered Molecular Aggregates: Motional Narrowing and the Effect of Intersite Correlations”. *J. Chem. Phys.*, **99 (11)**, (1993) 8466-8479.
- [17] Kamalov V.F., Struganova I.A., Tani T. and Yoshihara K., “Temperature Dependence of Superradiant Emission of BIC J-aggregates”. *Chemical Physics Letters*, **220 (3-5)**, (1994) 257-261.
- [18] Spano F.C, “ Nonlinear Optical Response of One-dimensional Molecular Crystals Breakdown of the Local Field Approximation”. *J. Chem. Phys.*, **96 (11)**, (1992) 8109-8116.
- [19] Spano F.C. and Mukamel S., “Superradiance in molecular aggregates”. *J. Chem. Phys.*, **91 (2)**, (1999) 683-700.
- [20] De Rossi U., Daehne S., Gomez. U. and Port. H., “Evidence for Incoherent Energy Transfer Processes in J-aggregates with Davydov Splitting”. *Chemical Physics Letters*, **287**, (1998) 395-402.
- [21] Scheblykin I.G., Bataiev M. M., Van der Auweraer M. and Vitukhnovsky A. G., “Dimensionality and Temperature Dependence of the Radiative Lifetime of J-aggregates with Davydov Splitting of the Exciton Band”. *Chemical Physics Letters*, **316 (1-2)**, (2000) 37-44.
- [22] Davydov A.S., “Theory of Molecular Excitons”. Plenum, New York (1971)

- [23] MacRae E.G. and Kasha M., "The Molecular Exciton Model in Physical Processes in Radiation Biology". Academic Press, New York (1964) 23-42.
- [24] Feldmann J., Herz A. H. and Regan T.H., "pH Dependence of Electronic and Nuclear Magnetic Resonance Spectra of Isomeric Cyanine Dyes". *J. Chem. Phys.*, **72** (6), (1968) 2008-2013.
- [25] Kuhn H., "J-aggregates". ed. Kobayashi(1996) 1-40.
- [26] Markovitsi D., Sigal H., Ecoffet C., Millié P., Charra F., Fiorini C., Nunzi J.M., Strzelecka H., Veber M. and Jallabert C., "Charge Transfer in Triaryl Pyrylium Cations. Theoretical and Experimental Study". *Chemical Physics*, **182** (1), (1994) 69-80.
- [27] Czikkely V., Försterling H.D. and Kuhn H., "Light Absorption and Structure of Aggregates of Dye Molecules". *Chemical Physics Letters*, **6** (1), (1970) 11-14.
- [28] Nolte H.N., "A Model of the Optically Active Scheibe-Aggregate of Pseudocyanine". *Chemical Physics Letters*, **31** (1), (1975) 134-139.
- [29] Scheibe G., "Optische Anregungen Organischer Systeme". Verlag Chemie, Weinheim (1966) 106.
- [30] MacRae E.G. and Kasha M., "Enhancement of Phosphorescence Ability Upon Aggregation of Dye Molecules". *J. Chem. Phys.*, **28**, (1958) 721-732.

- [31] Kenkre V.M. and Reineker P., "Exciton Dynamics in Molecular Crystals and Aggregates". Springer, Berlin (1982)
- [32] Frenkel J., "On the Transformation of Light into Heat in Solids.1". *Phys. Rev.*, **37 (10)**, (1931) 1276-1294.
- [33] Fidler H., Konester J. and Wiersma D., "Optical Properties of Disordered Molecular Aggregates: A Numerical Study". *J. Chem. Phys.*, **95 (11)**, (1991) 7880-7890.
- [34] Taylor C., el-Bayoumi A. and Kasha M., "Excited-state Two-proton Tautomerism in Hydrogen-Bonded n-heterocyclic Base Pairs". *Proceedings of the National Academy of Sciences of the United States of America*, **63 (2)**, (1969) 253-260.
- [35] Lakowicz L.J.R., "In Principles of Fluorescence Spectroscopy 2nd. Edition". Kluwer Academic/Plenum Publishers, New York (1999) 141-184, 187-193.
- [36] Van Amerongen H., Valkunas L. and van Grondelle R., "Some Optical Properties of the Excitonically Coupled Dimer in Photosynthetic Excitons". World Scientific, Singapore (2000) 73-138.
- [37] Parkash J., J H. Robblee, J. Agnew, Gibbs E., Collings. P., Pasternack
- [38] R. F. and de Paula J. C., "Depolarized Resonance Light Scattering by Porphyrin and Chlorophyll a Aggregates". *Biophysical Journal*, **74 (4)**, (1998) 2089-2099.
- [39] Fukutake N. and Kobayashi T., "Size Distribution of Pseudoisocyanine (PIC) J-Aggregates Studied by Near-field

- Absorption Spectroscopy". *Chemical Physics Letters*, **356 (3-4)**, (2002) 368-374.
- [40] De Barros R. B. and Ilharco L. M., "The Role of Cellulose Acetate as a Matrix for Aggregation of Pseudoisocyanine Iodide: Absorption and Emission Studies". *Spectrochimica Acta Part A: Molecular and Biomolecular Spectroscopy*, **57 (9)**, (2001) 1809-1817.
- [41] Kato T., Sasaki F., Abe S. and Kobayashi S., "Theoretical Study on the Absorption Spectra of Pseudoisocyanine Bromide (PIC-Br) Molecular J-aggregates". *Chemical Physics*, **230 (2-3)**, (1998) 209-221.
- [42] Scherer P. O. J. and Fischer S.F., "On the Theory of Vibronic Structure of Linear Aggregates. Application to Pseudoisocyanine (PIC)". *Chemical Physics*, **86 (3)**, (1984) 269-283.
- [43] Hanamura E., "Very Large Optical Nonlinearity of Semiconductor Microcrystals". *Physical Rev. B.*, **37 (3-5)**, (1988) 1273-1279
- [44] Ryzhov I. V, Kozlov G. G., Malyshev V.A, Knoester, J., "Low-temperature kinetics of exciton--exciton annihilation of weakly localized one-dimensional Frenkel excitons", *J. Chem. Phys.*, **114**, 5322-5329 (2001)
- [45] Lampoura S.S., Ph.D Thesis, "Dynamics in Biological Samples and J-aggregates Explored by Linear and Non-linear Optical Spectroscopy", Vrije Universiteit, 2001
- [46] Smith D.L., Luss H.R., *Acta Crystallogr., Sec. B* 28 (1972)

- [47] Delaney J., Morrow M. and Eckhardt C. J., "Observation of the J-band in the Crystal Spectra of Pseudoisocyanine (PIC)". *Chemical Physics Letters*, **122 (4)**, (1985) 347-351.
- [48] Van Burgel M., Wierma D.A., Duppen K., "The dynamics of one-dimensional excitons in liquids", *J. Chem. Phys* , **102 (1)**,(1995) 20-33
- [49] Burshtein K.Y., Bagatur'yants A.A., Alfimov M.V., "MO calculations on the Absorption Spectra of Organic Dimers. The Interaction Energy Between Dipole Moments of Electronic Transitions in Monomers and the Shape of Absorption bands", *Chemical Physics Letters*, **239**, (1995)195-200